Génie Mécanique

Mechanical Engineering

UNIVERSITÉ D'OTTAWA
UNIVERSITY OF OTTAWA

UNIVERSITY OF OTTAWA
Department of Mechanical Engineering

MATHEMATICAL MODELLING OF CASTING PROCESSES

by

M. Salcudean
Z. Abdullah

Final Report for the DSS Contract
22 ST.23440-0-9188/1

Ottawa, Ontario

April 18, 1987

93ff

ABSTRACT

This report describes the code SOLID-3, developed at the University of Ottawa to simulate liquid metal flow and heat transfer during casting processes. The program solves the conservation equations of momentum, mass and energy by the Finite Volume Method. The Boussinesq approximation is used to simulate the free convection occurring in the liquid metal. The velocities can be treated by three different techniques during solidification, the D'Arcy Source Method, the Fixed Velocity Method and the Increased Viscosity Method. Latent heat release is simulated by a source based method which can handle eutectic as well as isothermal solidification. Thermal contact resistance and gap formation are simulated at the mold casting interface. A number of different types of boundary conditions, for example fixed temperature, fixed heat flux or heat transfer coefficient with fixed ambient temperature can be imposed.

The code was tested by simulating the solidification of a cylindrical grey iron casting in a permanent mold. The mold was assumed to consist of a cast iron cylinder resting on a sand base with a gating system. A cast iron cover plate formed the upper part of the mold.

The results indicate that there is considerable liquid metal motion during the solidification process. This motion alters the temperature field in the liquid metal region and enhances heat transfer, resulting in faster cooling rates.

TABLE OF CONTENTS

1 ABSTRACT i

1 LIST OF FIGURES v

1 NOMENCLATURE vi

1 INTRODUCTION 1

2 LITERATURE REVIEW 5

2.1 Geometric Approaches 5

2.2 Numerical Approaches 8

2.2.1 Modelling of conduction heat transfer 8

2.2.2 Modelling of convective effects 10

2.2.3 Modelling of interface heat transfer 14

2.2.4 General purpose heat transfer codes used for solidification modelling 16

2.2.5 Latent heat formulations 17

3 MATHEMATICAL MODELLING 20

3.1 Governing Equation and Assumptions 20

3.2 Solution Procedure 21

3.3 Boundary Conditions 25

3.3.1 Fixed Heat Flux 26

3.3.2 Fixed Temperature 26

3.3.3 Mold Casting Interface 27

3.4 Latent Heat of Fusion 28

3.5 Velocity Treatment During Solidification 31

3.5.1 D'Arcy Source Method 31

3.5.2 Fixed Velocity Method 32
3.5.3 Increased Viscosity Method 33
4 SOFTWARE STRUCTURE 34
4.1 The MAIN program 34
4.2 Subroutine PRODEP 37
4.2.1 ENTRY SPECIF 37
4.2.2 ENTRY COOR 38
4.2.3 ENTRY RGRIDI 38
4.2.4 ENTRY GEOM 38
4.2.5 ENTRY INIT0 38
4.2.6 ENTRY BOUND0 39
4.2.7 ENTRY INPTD 39
4.2.8 ENTRY OUTPTD 39
4.3 Subroutine Latent 39
4.3.1 ENTRY CHKSOL 39
4.3.2 ENTRY UPLAT 39
4.3.3 ENTRY CALDHP 39
4.4 Subroutine PROMOD 39
4.4.1 ENTRY FRECON 40
4.4.2 ENTRY MODPRO 40
4.4.3 ENTRY ULOWER and ENTRY VLOWER 40
4.4.4 ENTRY MODU and ENTRY MODV 40
4.4.5 ENTRY UFIX0 and ENTRY VFIX0 40
4.4.6 ENTRY UDAR0 and ENTRY VDAR0 40
4.4.7 ENTRY MODP 40
4.5 Subroutine MODPHI 40

4.5.1 ENTRY FILOW 41
4.5.2 ENTRY MODFI 41
4.6 Subroutine INIT 41
4.6.1 ENTRY GRIDI 41
4.6.2 ENTRY GRIDP 41
4.6.3 ENTRY GRIDV 41
4.6.4 ENTRY GRIDT 41
4.6.5 ENTRY SET 41
4.6.6 ENTRY SETSTR 41
4.7 Subroutine PRINT 41
4.8 Subroutine LISOLV 42
4.9 Subroutines CALCU, CALCV and CALCFI 42
4.10 Subroutine CALCP 42
4.11 Subroutine HYBRID 42
4.12 Subroutine CORESI 42
4.13 Subroutine ERROR 43
4.14 Subroutines PREAD and PWRITE 43
4.15 Subroutine SOZONE 43
4.16 Subroutine INCO 43
5 SOLUTION OF A TEST CASE 44
5.1 Problem Assumptions and Boundary Conditions 44
5.2 Results and Discussion 47
5.3 Conclusions 49
5 REFERENCES 50

LIST OF FIGURES

1 Grid arrangement for the Finite Volume Method 61
2 Non-uniform grid specified on a rectangular domain 62
3 Grid cells at the mold casting interface 63
4 Solid, mushy and liquid zones 64
5 Simplified flowchart of SOLID-3 65
6 Schematic of the mold and mesh used 66
7 Thermal contours and velocity field in the casting 67
8 Temperatures at casting midsection 68
9 Temperatures at casting centerline 69
10 Heat transfer coefficients at the mold casting interface 70

NOMENCLATURE

a	- nodal coupling coefficient
A	- area
B	- very large number
C	- specific heat
F	- free convection heat transfer coefficient
g	- interface contact fraction
h	- sensible enthalpy ($C \times T$)
H	- heat flux
h^*	- equivalent heat transfer coefficient
	- for conduction and radiation at gap
k	- constant in Chvorinov's Rule or thermal conductivity
p	- pressure
Pe	- cell Peclet number
Q	- latent heat release
r	- radial coordinates
R	- thermal contact resistance at mold casting interface
S	- casting surface area or source term
s	- solid fraction
Sp	- part of source term which is coefficient of ϕ_P
Su	- constant part of source term
t	- time
T	- temperature
u	- velocity along x (or axial) direction

v	- velocity along y (or radial, r) direction
V	- cell volume
x	- axial coordinates
$\partial x, \partial r$	- partial derivatives in the
	- x,r directions respectively
V	- casting volume

Greek Symbols

ϵ	- emissivity
η	- porosity
ϕ	- general variable
Γ	- diffusive coefficient
μ	- viscosity
ρ	- density
ψ	- stream function
σ_b	- Stefan-Boltzmann constant
ω	- vorticity

NOTE: Other symbols are defined where they are used.

INTRODUCTION

Computer aided techniques are important to the design of castings and to casting production for many economic as well as practical reasons. Canada's foundries serve over 90% of the durable goods industry, and show net annual sales of over 1.5 billion dollars [1,2]. Traditionally, the details of the production techniques of casting designs have been left in the hands of skilled and experienced foundrymen, however if the industry is to maintain it's competitive position in the world market, it has to supplement these skills with a more scientifically based approach.

In a typical casting process liquid metal is poured into a mold, solidification takes place, the casting cools down and is ejected from the mold. The mold is usually made of sand or metal. When a metallic mold is used, the process is termed as permanent mold casting. This process has already gained wide acceptance for non-ferrous alloys and is coming into increasing use for cast iron. Equipment and procedures needed to reduce environmental hazards associated with sand molding are making that process ever more costly, and the excellent dimensional consistency and good surface finish obtainable with permanent molding are increasingly attractive as customer demands on castings become more stringent. From a heat transfer point of view, the permanent mold casting cycle can be roughly divided into three stages:

1)The Filling Transient.

This stage extends from the beginning of the cycle when pouring begins to the time when the mold fills up and pouring of the liquid metal is completed. This stage of the process is neglected completely in the literature, for example, [3-21] and researchers assume that the mold fills up instantaneously. In reality, this stage of the cycle can be very important because of the following reasons:

a) A significant amount of convection takes place in the liquid metal due to the

incoming jet. This has the effect of "mixing" the liquid metal and equalizing the temperatures in the liquid metal [22].

b) The liquid metal convection influences the distribution of solutes (for example, inoculants) resulting in segregation defects [23].

c) The finite time period required for the filling transient causes the liquid metal to be in contact with the bottom region of the mold for a longer period of time than the top, increasing the asymmetry of the temperature distribution in the mold. The non-symmetric temperature distribution in the mold causes increased thermal stresses, possibly reducing mold life [24]

d) Solidification can start close to the mold walls even during pouring if the temperature of the mold is low enough.

e) The velocity and temperature distributions at the end of the filling transient are required for modelling as they represent the correct initial conditions for the next stage of the casting cycle.

2)The Solidification Process

In this stage of the casting process cooling and solidification of the liquid metal takes place. Natural convection occurs as long as there are temperature gradients in the liquid metal. The flow patterns may depend on the initial velocities generated due to the inflow jet (described in stage 1). Solidification continues and the solidus front advances into the liquid metal. If a pure metal is freezing the solidification takes place at a unique temperature and the solidus-liquidus interface is *sharp*. In the case of solidification of alloys, the metal solidifies over a range of temperatures and there is a ***mushy*** region between the solidus and the liquidus interfaces. Natural convection stops when the thermal gradients in the liquid metal disappear and the temperature becomes uniformly equal to the liquidus temperature. During this stage of the process, a gap may form at the mold casting interface. This gap forms

because the casting contracts and the mold expands thermally. The heat transfer through the "air" gap at the mold-casting interface is a complex phenomenon, consisting of conduction through the air, conduction at spot contacts and radiation between the mold and casting walls. The solidus (and liquidus in case of alloys) interfaces continue to advance into the liquid metal and eventually the entire casting solidifies. The metal shrinks during the phase change, and if fresh liquid metal is not available to account for the shrinkage, a cavity or a porous area may form inside the casting. Stage two of the process ends when the solidification of the entire casting is complete.

3) Post Solidification Cooling.

During this stage the casting cools in the mold. Heat transfer during this stage is through conduction. In commercial production runs, this stage of the process is often bypassed entirely, and the casting is removed from the mold as soon as a thick enough shell has solidified to contain the liquid metal core. The mold can then be used again for next casting cycle.

The heat transfer mechanisms during the casting processes described previously are numerous and very complex. Mathematical modelling of these processes can potentially improve our level of understanding and can aid in the design of both the casting and the mold. The objective of such simulation is to develop mathematical models and subsequently, CAD (Computer Aided Design) tools which would provide the casting engineer with information on the location and movement of the solid-liquid interface in the solidifying alloy, and on temperature distributions as functions of the various operating parameters and time.

This report introduces the code "SOLID-3" which can model liquid metal flow and heat transfer during the solidification process. The code is quite general and can solve a large variety of problems. This program has been developed by the

modification of "TEMA" [97] of the University of Ottawa, which is a three dimensional, transient fluid dynamics code. The objective of this report is to outline the essential features and structure of SOLID-3 to the intended user. It is assumed that the user of this code has a basic understanding of the Finite Volume Method, for which he is referred to Patankar [95].

SOLID-3 solves the finite volume approximations to the governing partial differential conservation equations of fluid flow and heat transfer within the problem domain. The field values of the temperature, pressure, density and velocities are obtained by transforming the differential equations by the Finite Volume Method to produce algebraic equations linking the dependant variable at each node to it's neighbors and to the value at the previous time step. The code is fully implicit in time, which allows relatively large time steps to be taken without onset of instability. A hybrid differencing scheme in space is used which allows a wide range of velocities.

This report is divided into five chapters. A detailed survey of solidification modelling techniques that are currently available in the literature is presented in chapter 2. The mathematical formulation of SOLID-3 is outlined in chapter 3. The software is described in chapter 4. Chapter 5 presents a test case and some typical results with interpretation.

2 LITERATURE REVIEW

2.1 Geometric Approaches

Solidification phenomena during casting processes have been studied for a long time. Before the present stage of advancement of the capabilities of digital computers, most of the research was focussed on geometric simulation techniques. Geometric models correlate the solidification time of castings to basic characteristic dimensions of the casting (for example, the diameter and height of cylindrical castings). Usually extensive experimental data is required to obtain these correlations, and they are, to a great extent, fairly limited to the shape of the castings from which the experimental data is obtained. One very useful set of information that can be obtained is the *relative* solidification times or the solidification patterns for different castings. The solidification patterns can show the region where solidification takes place last. Depending on the liquid metal feeding paths available to this region, one can determine if there will be a cavity (shrinkage) at this location. This information is critical to the casting designer and it can be obtained at a relatively low cost.

The pioneering work in the geometrical modelling of solidification was done by Chvorinov [25], who derived a simple relation known as the "Chvorinov's Rule" and stated as:

$$t = k \times \left(\frac{V}{S}\right)^2$$

In this relationship "t" is the *total* solidification time of a casting, "V" is the volume,"S" is the surface area and "k" is a constant usually determined by fitting this equation to experimental data. This equation was originally proposed for casting and ingots of cylindrical shape but was subsequently used widely in the analysis of castings of general shape. The basis of this relationship can be easily appreciated if the volume of a casting is related to it's heat content and the surface

area is related to the rate of heat extraction. The constant "k" takes into account the combined effects of the thermophysical properties and geometry of the casting and the mold. This relation is usually only applied to pure metals which solidify isothermally and in sand molds where the temperature at the mold casting interface is fairly constant during solidification.

Heine [26] used this ratio to determine the relative freezing times for various regions of castings by considering each region separately. He showed that regions of high "$\frac{S}{V}$" freeze in a very short time while regions of low "$\frac{S}{V}$" take longer to freeze. He determined the order of solidification of different regions of the casting from this ratio, assuming that the constant "k" is the same for all the regions of the casting. The order of freezing of the different regions of the casting provided insight in the freezing paths and probable shrinkage cavity locations.

Mertz and Heine [27,28] investigated feeding distances and solidification times of various casting shapes and related them to $\frac{S}{V}$. Loper and Kotschi [29] used Chvorinov's rule to develop a series of graphs relating the *relative* solidified thickness versus characteristic dimensions (for example, plate thickness, boss diameter) of the castings to provide quick design assistance to foundrymen. One of the major limitations of their work was that they assumed an infinite mold thickness. Their work was extended by Nehru, Nagajunasagar, et al [30] for Copper and gun metal castings, and for finite mold wall thicknesses by the introduction of a parameter "VR" defined as the ratio of the mold wall thickness to casting wall thicknesses. Kotschi and Loper [31] then extended this concept to include the effects of chills by including additional factors in the Chvorinov's rule to take into account the different thermal properties of chills and mold materials.

Koteschi, Loper et al [32] demonstrated the basic design steps required to eliminate shrinkage defects in a cover plate casting by using the geometric technique. Kotschi and Plutshack [33] showed how lines of constant "$\frac{V}{S}$" called the "K-contours" could be plotted in the casting domain. These lines represent the advancement pattern of the solidification front and can hence be used for predicting defects. Kim [34] developed software which produced K-contours in simple "L, T, X, V, Y" sections. By combining these sections in various combinations he could predict the solidification patterns in castings of many shapes. He did extensive experimental work using mainly the "pour out technique" in Aluminum castings. In this method the liquid metal in partially solidified castings is poured out to investigate the advancement of the solidification front at the various stages of solidification.

Mohan and Shenoy [35] included additional terms in the basic Chvorinov's Rule to extend it to include modelling solidification in permanent molds by considering the effects of mold wall thickness, physical properties of the mold and coating on the mold walls.

While the geometrical method has the advantage of showing the propagation of the solidification front, it does not provide any information about the actual solidification times. This information is required to determine the time at which the casting should be removed from the mold. This method cannot improve our detailed understanding of the heat transfer processes involved because of it's inherently simple nature. The liquid metal convection effects, the interfacial heat transfer phenomena, the thermophysical properties of the castings, molds and chills, the effects of various initial and boundary conditions are all neglected. This leads to over simplification of the actual process and loss of accuracy of the results.

2.2 Numerical Approaches

Numerical simulations of the casting processes have now become very popular [3-21,41-61]. In these simulations the governing equations of heat transfer are solved numerically after simplifications on the basis of various assumptions. These models offer a higher level sophistication and a lot of information, for example heat transfer rates, temperature distributions etc.. The limitations of these models are that the computationally economical models often involve unrealistic simplifying assumptions, while the "physically realistic" models are very expensive to run. These models also need detailed heat transfer parameters such as thermal conductance, density, specific heat, latent heat, pouring temperature and fluid properties in case liquid metal motion is to be modelled. At present, the literature sorely lacks detailed thermophysical properties of liquid metals. The numerical models do provide important information, and are invaluable in the detailed study of casting processes. With computation cost steadily decreasing the trends indicate that numerical models are gaining the upper hand in popularity [14,15]

2.2.1 *Modelling of conduction heat transfer*

Some of the early work in computational modelling was done by Lazardis [3,4] who used the explicit finite difference scheme to solve the equation of heat conduction for one and two dimensional forms for the solidification of a semi-infinite slab. He showed that the rate of solid/liquid interface advance was a function of the temperature gradients in the liquid and the solid at the interface and the latent heat of fusion. Finite difference equations were then developed and substituted into the energy conservation equation defining the rate of movement of the interface. The physical properties were assumed to be constant and the latent heat was assumed to be released isothermally. Pehlke, Kirt et al [5] and Jeyarajan and Pehlke [6] solved the heat conduction equation two dimensionally (in cartesian and cylindrical

coordinates) to simulate the solidification of Silicon Brass alloys and Aluminum in sand molds. The latent heat of fusion was incorporated in the specific heat. Davies [7] found an explicit solution of the transient heat conduction equation to determine heat flow and feeding range in the runners of sand molds. The latent heat was incorporated in an enthalpy formulation. Reddy [8] solved the heat conduction equation for the simulation of V shaped Al-Cu castings in sand molds. The latent heat release was simulated by a post iterative integration technique. Brody and Stoehr [9] and Stoehr [10] discussed the application of the explicit solution of the heat conduction equation to problems of casting and welding. Clyne [11] developed an explicit finite difference formulation for a one dimensional solution of heat conduction with latent heat released over a range of temperatures. Ohtsuka, Mizuno, Yamada [12] found the explicit solution of the heat conduction due to solidification of Aluminum alloy castings in Steel molds. A thermal contact resistance between the casting and the mold was simulated. Zeng and Pehlke [13] solved the heat conduction equation governing the heat transfer during the solidification of cylindrical brass castings. An explicit method was used. Pouring time was simulated without natural convection. Thermal contact resistance and an air gap formation after a certain gap formation time was also simulated.

Marrone, Wilkes and Pehlke [14,15] solved the heat conduction equation for the solidification of 'T' and 'L' shaped steel in sand molds. Both the Saul'yev explicit finite difference approximation and the Alternating Direction Implicit Method were used for the solution. Jeyarajan and Pehlke [16] used the same method to study the solidification of cylindrical Aluminum alloy castings in sand molds. Low [17] used the Alternating Direction Implicit Method to solve the heat conduction equation for square and cylindrical ingots. Pouring time and thermal contact resistance were not modelled. The latent heat release was modelled by the Modified Specific Heat

method.

Weatherwax and Riegger [18] and Abis [19] used finite element techniques to solve the heat conduction equation for the solidification of Aluminum castings in three dimensions. The latent heat release was modelled with the Modified Specific Heat method. Hong, Umeda and Kimura [20,21] applied the boundary element method to study the solidification phenomena. The latent heat of fusion was taken into account by post iterative temperature adjustment methods.

2.2.2 *Modelling of convective effects*

The convective flow that is developed in the melt during pouring and solidification has received relatively little attention until very recently. The liquid metal flow due to pouring and during natural convection in the melt because of thermal gradients is very important as it can have a large effect on the heat transfer, resulting in an influence on the structure of the solid formed and the rate of solidification [36]. In multi-component systems, the natural convection occurring in the melt can also affect the distribution of the solutes in the system [37]. Cole and Bolling [36] have suggested that the grain structure of an ingot can be controlled if the relative motion of the liquid metal is controlled.

Huang [38] has proposed a closed form analytical solution to the one dimensional momentum equation for the solution of the melting problem for a vertical semi-infinite region. The Boussinesq model of the density is used in the momentum equation and the standard Neuman solution is used for the temperature distribution. In the Boussinesq model the fluid is treated as incompressible for all purposes except for the calculation of the buoyancy forces due to thermal gradients. This model is generally used in numerical methods to compute natural convection in incompressible liquids.

Goodling and Khadar [39] solved the one dimensional conduction equation with

a convective boundary condition at the solidus liquidus interface. The equation was cast in a dimensionless form for cartesian, cylindrical or spherical coordinate systems. The convective heat transfer coefficient at the solidus liquidus interface was found to be important in determining the solidification rate. Gau and Viskanta [40] conducted a one dimensional analysis of freezing of a solid in a rectangular cavity. They modelled the natural convection heat transfer coefficient at the solid liquid interface by steady heat transfer correlations for cavities without phase change. The heat conduction equation in the solid region was solved by an integral technique. The solution in the liquid region was not obtained.

Hirt [41] showed how the SOLA algorithm could be used for the computation of liquid metal flow patterns during foundry processes. Stoehr and Hwang [42] have also used the Marker and Cell method to predict the flow of metal into a rectangular mold cavities. Wilkes and Smith [43] solved the Navier Stokes equations in cylindrical coordinates to simulate the free surface flow of a fluid issuing vertically upwards from the base of a vertical cylindrical cavity. They used the Marker and Cell technique in conjunction with the Dufort-Frankel finite difference approximation in the primitive variable approach. The energy equation and solidification were not solved in any of the works mentioned in this paragraph.

Sparrow, Patankar and Ramadhyani [44] studied melting of a solid around a semi infinite vertical pipe, imbedded in the solid and heated above the fusion temperature. The fluid flow due to natural convection and heat transfer in the melt was analyzed. An implicit, primitive variable formulation was used with a moving mesh (in a transformed coordinate system) which conformed to the solid liquid interface. The movement of the interface due to melting was computed explicitly at the end of each time step.

Stream function / Vorticity based methods are also gaining popularity for the

computation of natural convection in enclosures [23,45-47]. The stream function is defined as ψ where

$$u = \frac{\partial \psi}{\partial y}$$

$$v = -\frac{\partial \psi}{\partial x}$$

and the vorticity is defined as

$$\omega = \frac{\partial v}{\partial x} - \frac{\partial u}{\partial y}$$

Substitution of the stream function and the vorticity expressions after differentiation of the momentum equations in their primitive variable form results in elimination of the pressure gradient terms. This has the advantage that iterations to correct the pressure field to satisfy continuity are no longer required as continuity is automatically satisfied. The disadvantages of this formulation are that:

a) Extension to three dimensions is difficult.

b) Application of the boundary conditions is more involved.

c) The method has somewhat less physical appeal as compared to the primitive variable formulation.

Kublbeck, Merker and Straub [23], and Wilkes and Churchill [45] used the vorticity formulation in conjunction with the Peaceman and Rachford [46] Alternating Direction Implicit method to solve the momentum and energy equations for natural convection in rectangular geometries. The ADI method allows relatively large time steps with a numerically efficient tri-diagonal formulation. Kee and McKillop [47] also used the same formulation, but for cylindrical geometries with asymmetric boundary conditions at the circumference. Ozoe, Mouri et al [48] computed two dimensional natural convection in rectangular sections for both laminar and turbulent natural convection. The turbulence modelling was done by using the $k - \epsilon$ turbulence model. Solidification was not modelled in any of these works.

Szekely and Yadoya [49], and Kroeger and Ostrach [50] solved the fluid flow coupled with natural convection for continuous casting systems. Szekely and Yadoya [49] used the primitive variable implicit method, however the solidification was not solved. Kroeger and Ostrach [50] used the stream function vorticity approach with a moving grid to conform to the solid/liquid interface. A "guess and correct" procedure was used to determine the position of the solid liquid interface.

Guenigault [51] studied solidification inside spheres and tubes using the stream function formulation. Isothermal latent heat release was assumed with constant thermophysical properties. Ramachandran, Gupta and Jaluria [37] solved the solidification problem in a rectangular two dimensional enclosure with adiabatic top and bottom boundaries. The fluid flow was solved via a stream function vorticity formulation and the ADI technique was used for the solution. A moving mesh was used to track the solid liquid interface. The density variation causing the natural convection was handled by the Boussinesq approximation.

Desai, Kim [52], and Desai, Berry, Kim [53] used the finite element method with the stream function vorticity technique to model the advancing liquid metal front in runner channels and the free convection in molds. The advancing front of the liquid metal in the runner was handled by a deforming mesh. The solidification of the liquid metal was not modelled. The work was done for a simple two dimensional rectangular runner shape for laminar flow.

Voller [54,55] used the Patankar and Spalding finite volume method [56] in a simple coarse mesh to model free convection fluid flow and solidification. Fictitious material properties with Dirichlet type boundary conditions were used. The latent heat release was modelled by a source based method.

The above mentioned works that have dealt with solidification have all considered the solidification of pure materials which have a unique solidification temper-

ature. In practice, the solidification of alloys is also very common in the industry. In the solidification of alloys, a two phase or *mushy* zone exists between the solid and the liquid regions. Liquid metal flow in this zone has also been studied by a number of researchers, for example [57-59].

Stewart and Weinberg [57] have experimentally studied the penetration of liquid metal into the mushy zone for Tin Lead alloys. The depth of penetration was studied by radioactive tracer techniques. Gabathuler and Weinberg [58,60] also investigated the penetration of liquid metal into the mushy zone by radioactive tracer methods for Aluminum alloys with Silicon, Copper and Magnesium. In both of these studies the researchers found that the penetration of the liquid metal was small as compared with the thickness of the solid liquid interface. The penetration was found to increase with an increase of the velocities in the liquid zone. Maples and Poirier [59] treated natural convection inside the mushy zone as flow through a porous medium.

2.2.3 *Modelling of interface heat transfer*

A very important aspect of heat transfer during casting processes, especially during permanent mold casting is heat transfer at the mold casting interface. The interface thermal resistance is considered to be one of the primary factors controlling the heat flow [61-66].

Ho and Pehlke [61-64] experimentally measured the heat transfer at the mold casting interface between an Aluminum casting and a Copper chill in a sand mold. The experimental setup was designed such that the heat flow was one dimensional. Temperatures in the chill and the casting and the interfacial gap were measured. The inverse heat conduction problem was solved to find the interfacial heat transfer. Theoretical models were then developed for the casting mold interfacial heat transfer. Their models divided the heat transfer at the gap into two components,

radiative between the casting and chill walls and conductive through the air in the gap. The author neglected to model the interface heat transfer before gap formation, claiming that the gap formation time for their experiments is in the order of 10^{-3} seconds. The heat transfer due to conduction through direct spot contacts was also neglected because of the additional resistance of oxide films and scale at the contacting surfaces.

Sully [65] and Srinivasan [66] studied the heat transfer through the casting mold interfaces for various casting and mold materials, sizes and shapes. Their work was experimental. Their results indicated that the value of the interface heat transfer coefficient first increases from a low value to a peak value (as the hydrostatic pressure increases during pouring) and then it decreases rapidly (as a solidified skin forms and the casting wall moves away from the mold). The interface heat transfer coefficient value was also found to have time dependant values which were relatively insensitive to mold or chill material and temperature. The values were found to be strongly dependant on the temperature of the casting and its geometry (shape). The solidified inflow gates and protruding sections of the casting hold it against certain mold cavity surfaces, increasing the interface heat transfer. This effect has been confirmed recently by Abdullah et al [22].

Majumdar, Raychaudhuri and Dasgupta [67] developed a new technique in which they measured the electrical capacitance of the air gap and from it determined the gap width.

Sun [68] proposed a simple expression for the interfacial heat transfer coefficient by considering only heat transfer due to conduction at the interface. Gap formation was not modelled.

Thamban and Panchanathan [69] solved the unidirectional solidification of Aluminum assuming various heat transfer coefficients and determined the correct inter-

facial heat transfer coefficient value by comparing their results with experimental data. This technique was also used by Davies [70] and Nishida and Matsubara [71] in which experiments of unidirectional solidification in cylindrical mold were carried out and the heat transfer was simulated numerically. The values of the gap heat transfer coefficient that yielded good agreement with the experimental data were considered to be applicable.

Yovanovich [72], and Yovanovich et al [73,74] have proposed correlations to predict interfacial heat transfer. A random distribution of asperities with a Gaussian height distribution is assumed for the contacting surfaces. Heat transfer due to spot contact and due to conduction through the air in the gaps is considered.

2.2.4 *General purpose heat transfer codes used for solidification modelling*

Many general purpose codes are now available for simulation for heat transfer during casting processes [75-80]. All of these codes model only conduction heat transfer, completely neglecting convective effects. The most widely used of these codes are the CINDA and SINDA family of codes originally written for NASA by the Chrysler Corporation and TRW Inc respectively. This family of codes uses the thermal analog approach in which the thermal functions are equated to the corresponding electrical analogs. The heat flow problem is then solved in an analagous manner [78]. The latent heat release is calculated by post iterative heat accumulation methods. The codes can handle one, two or three dimensional problems. MITAS is basically the same as CINDA but has been developed for CDC computers by the Martin-Marietta Corporation [79].

TRUMP is a general purpose finite difference code developed by the Lawrence Radiation Laboratory [77,80]. It can handle multidimensional heat conduction problems. The latent heat can be taken into account using an enthalpy formation. AYDER is a two dimensional finite element code developed by the Los Alamos Scientific

Laboratory [79]. It has the limitation that the latent heat can only be simulated by an equivalent specific heat method. ANSYS and MARC are two one, two and three dimensional finite element codes developed by Swanson Analysis. They are both moderately expensive to run; MARC can deal directly with latent heat but ANSYS needs external manipulation [75]. CAST has been developed by the Abex Corporation and is a three dimensional fully explicit code [77]. Latent heat evolution can be modelled by the equivalent specific heat method. The main strength of CAST is that it can present results in the form of a colored map, each color representing a range of temperatures. This technique gives the results a unique physical appeal. A code has also been developed at the Department of Mechanical Engineering, University of Ottawa [81,82]. This code uses the ADI method to solve two dimensional heat conduction problems in cartesian and cylindrical options. The code can simulate latent heat release by either the equivalent specific heat method or by a post iterative heat integration method. Air gap formation, thermal contact resistances and mold cooling channels can also be modelled. It is possible to obtain output in the form of colored map format. The mathematical basis of this code has been described in previous reports [—], and a user's manual is presented in Vol. 1 of this report.

2.2.5 *Latent heat formulations*

There are numerous techniques of tracking the moving phase front and latent heat release, however many of these will not be discussed here as they are limited to one dimensional idealized situations and are computationally too expensive to be implemented in multidimensional modelling.

The most widely used formulations to account for latent heat release in multidimensional solidification modelling are the "Apparent Heat Capacity" method, the "Heat Integration" method and the "Enthalpy Formulation" method.

The Apparent Specific Heat Method [83,88] is a very simple technique in which the latent heat is included in the specific heat of the material. An apparent specific heat is defined in the range of the phase change temperatures to account for the entire enthalpy change, including both the sensible as well as the latent heat.

The advantages of this formulation are that it is numerically very economical, it is very simple to implement and its predictions of the spatial position of the phase front are quite accurate. The disadvantages are that it cannot handle isothermal solidification or freezing that takes place over a very narrow temperature range. Also, small time steps are needed to correctly account for the enthalpy change during solidification.

In the Heat Integration Method [81-83,88,90], the temperatures of all the nodes are monitored. As soon as the temperature of any node drops below the freezing temperature, it is considered to be undergoing phase change. An accounting for the energy lost by the node at each cycle is set up and at the end of each cycle the nodal temperature is reset to the freezing temperature. The energy lost by the node is monitored until it is equal to the latent heat. At this point a flag is set, indicating that the node has "solidified". In the subsequent cycles the temperature of the node is allowed to fall in the usual manner.

The advantages of this method are that it can be used very easily in multidimensional modelling, with isothermal or non-isothermal phase change and arbitrary time step.

A disadvantage of this method is that the phase front is not continuously followed which can lead to inaccuracies near the phase change locations. Another disadvantage is that an elaborate system of accounting and indexing has to be maintained for each node.

In the Enthalpy Formulation Method [91-96] the energy equation is formulated

with enthalpy as the dependant variable rather than the temperature. After the solution of the energy equation, the temperature is redetermined, taking the latent heat into account.

3 MATHEMATICAL FORMULATION

3.1 Governing Equation and Assumptions

The general transport equation can be written for the axi-symmetric cylindrical coordinate system as:

$$\frac{1}{r}\Big[\frac{\partial}{\partial x}(\rho u r\phi) + \frac{\partial}{\partial r}(\rho v r\phi) - \frac{\partial}{\partial x}(r\Gamma_\phi \frac{\partial \phi}{\partial x}) - \frac{\partial}{\partial r}(r\Gamma_\phi \frac{\partial \phi}{\partial r})\Big] = S_\phi + \frac{\partial \rho \phi}{\partial t} \qquad (1)$$

where ϕ is the general variable representing u, v and h, Γ_ϕ is the appropriate diffusive coefficient of ϕ and S_ϕ contains the applicable source terms. Table 1 lists Γ_ϕ and S_ϕ for different ϕ.

Table 1

QUANTITY	ϕ	Γ_ϕ	S_ϕ
Continuity	1		0
Radial Momentum	v	μ	$-\frac{\partial p}{\partial r} - \frac{2\mu v}{r^2} + S^v$
Axial Momentum	u	μ	$-\frac{\partial p}{\partial x} + S^u$
Energy	h	$\frac{k}{C}$	Q

In the above table S^u and S^v are diffusive terms given by:

$$S^u = \frac{\partial}{\partial x}(\mu \frac{\partial u}{\partial x}) + \frac{1}{r}\frac{\partial}{\partial r}(r\mu \frac{\partial v}{\partial x}) \qquad (2)$$

$$S^v = \frac{\partial}{\partial x}(\mu \frac{\partial u}{\partial r}) + \frac{1}{r}\frac{\partial}{\partial r}(r\mu \frac{\partial v}{\partial r}) \qquad (3)$$

The differential equations arrived at by the substitution of the various ϕ s have to be solved to determine the velocity field in the liquid metal and temperature field in the casting and mold during the solidification process.

3.2 Solution Procedure

The solution procedure adopted for the problem is based on a primitive variable technique, specifically the Finite Volume Method [95,97]. Other techniques, for example, stream function-vorticity formulations [45-47] and the Eularian Lagrangian Method [100-102] were examined for the modelling of liquid metal flow and heat transfer in casting processes. The basic problem with stream function-vorticity formulations is that the boundary conditions are difficult to specify and extension to three dimensions is difficult. The Eularian Lagrangian Method is an extension of the Marker and Cell method originally developed at Los Alamos Laboratories [41]. This method is explicit and suffers from severe time step limitations. At it's present level of development, this method would need array processor facilities to model a typical casting process in a reasonable time period. This requirement makes the method impractical for EMR at present and for this reason the Finite Volume Method was chosen. This method has been embodied in the SOLID-3 code and has the following features:

(i) A finite difference procedure is used in which the dependant variables are the pressure, the velocity components and the sensible enthalpy (defined as the product of the temperature and the specific heat).

(ii) The procedure involves a "staggered grid" (please refer to Fig. 1) in which scalar quantities are defined at the nodal points and the velocities are defined at the cell walls.

(iii) A line by line relaxation technique is used for the solution of the algebraic equations. The TDMA (Tri-Diagonal Matrix Algorithm) is used to solve the matrix set which results for each grid line.

The Finite Volume Method has been discussed in detail by Patankar [95]. The basic steps of the method can be summarized as follows:

1) The continuity equation is solved using given u and v fields, which yields corrections for the pressure and velocity fields.

2) The corrected velocity fields are used in the solution of the algebraic equations for the enthalpy field.

3) The solution of the enthalpy field yields body forces via the Boussinesq approximation. The momentum equations are solved again using these body forces to produce updated velocity fields.

4) Steps (1) to (3) are repeated until convergence.

The Finite Volume Method has the advantage that it is implicit in time, therefore relatively large time steps can be taken without instability. All the linkages in the algebraic equations provide a high degree of flexibility so complex flow fields can be simulated. The difficulties in the solution spring mainly from the interlinkages between the different ϕ s. One of these is the linkage between the velocity components, which occurs through the unknown pressure field and through the conservation equation. The coupling between the temperature and the velocity fields is especially important during the simulation of solidification because the liquid metal flow is buoyancy driven. This causes a two-way coupling between the momentum and energy solutions which makes the computations very prone to divergence. In addition, special treatment has to be applied to simulate latent heat release and a moving solid-liquid interface. All of these complexities lend a peculiar flavor to solidification modelling and to computational fluid dynamics in general, but they can also result in long periods of frustration if one is not very careful in the specification of boundary conditions and other problem parameters.

The finite difference equations are solved on a mesh shown in Fig. 1. The scalar quantities, for example the nodal sensible enthalpies, the pressure and the nodal latent heat content are defined at the *nodes*, which are at the cell geometric centers.

The point "P" is a node and it's north, south, east and west neighbors are "N, S E, W" respectively. The velocities are defined at the cell walls between the pressures which "drive the flow". This grid arrangement is required to prevent wavy and unrealistic velocity fields [95]. The control volumes representing the velocities are also shown in Fig. 1.

The first step in the derivation of the finite volume equations is the integration of $eq(1)$ over the appropriate control volume (centered around the ϕ). The resulting equation is:

$$\left[\rho u\phi - \Gamma_\phi \frac{\partial \phi}{\partial x}\right]_e A_e - \left[\rho u\phi - \Gamma_\phi \frac{\partial \phi}{\partial x}\right]_w A_w + \left[\rho v\phi - \Gamma_\phi \frac{\partial \phi}{\partial r}\right]_n A_n$$

$$- \left[\rho v\phi - \Gamma_\phi \frac{\partial \phi}{\partial r}\right]_s A_s = [Sp\phi_p + Su]V \qquad (4)$$

where the lower case subscripts "n, s, e, w" refer to the north, south, east and west faces of the computational cell. Sp and Su are linearized source terms shown in Table 2.

Table 2

QUANTITY	ϕ	Γ_ϕ	Sp_ϕ/V	Su_ϕ/V
Continuity	1	0	0	0
Radial Momentum	v	μ	$-\frac{2\mu}{r^2}$	$-\frac{\partial p}{\partial r} + S^v$
Axial Momentum	u	μ	0	$-\frac{\partial p}{\partial x} + S^u$
Energy	h	$\frac{k}{C}$	0	Q

The diffusion terms S^v and S^u in the above table are defined by $eq(2)$ and $eq(3)$.

A stabilization technique is used in which a false source is added on to each algebraic equation. The magnitude of this false source is:

$$S_{false} = |m_{net}|(\phi_P{}^o - \phi_P) \tag{5}$$

where m_{net} is the net flow out of the cell and the superscript "o" stands for the previous iteration value. This false source tends to make the equation set more diagonally dominant in the initial cycles and helps stabilize the solution. At convergence ϕ_p and $\phi_p{}^o$ are equal so the false source disappears.

The next step is to evaluate the convective diffusive terms, $[\rho u\phi - \Gamma_\phi \frac{\partial \phi}{\partial x}]$ in $eq(4)$, at the faces of the cells. The hybrid differencing scheme is used to express these in terms of the nodal ϕ values. This scheme uses central differencing if the convection through the cell is low ($|Pe| \leq 2$), and upwind differencing if the convection through the cell is high ($|Pe| > 2$). The cell Peclet number, Pe, is defined as

$$Pe = \frac{(\rho u)\delta x}{\Gamma_\phi} \tag{6}$$

The convective diffusive term for the east face of the cell,

$$C_e = [\rho u\phi - \Gamma_\phi \frac{\partial \phi}{\partial x}]_e \tag{7}$$

for example, can be represented by the hybrid difference scheme as

$$C_e = \begin{cases} (\rho u)_e A_e \frac{(\phi_P + \phi_E)}{2} - \Gamma_\phi A_e \frac{(\phi_E - \phi_P)}{\delta x_e} & \text{for } |Pe| \leq 2 \\ (\rho u)_e A_e \phi_P & \text{for } Pe > 2 \\ (\rho u)_e A_e \phi_E & \text{for } Pe < -2 \end{cases} \tag{8}$$

where the Peclet number is evaluated on the east face of the cell. In a similar manner all the cell facial fluxes in $eq(4)$ can be expressed in terms of the nodal value ϕ_P and the neighbor values ϕ_N, ϕ_S, ϕ_E and ϕ_W.

After expressing the cell facial fluxes in $eq(4)$ in terms of the nodal ϕ values and collecting the coefficients of ϕ_P, ϕ_N, ϕ_S, ϕ_E and ϕ_W the following algebraic equation is obtained

$$a_P\phi_P = a_N\phi_N + a_S\phi_S + a_E\phi_E + a_W\phi_W + Sp\phi_P + Su \tag{9}$$

In the above equation a_P, a_N, a_S, a_E and a_W are the collected coefficients of ϕ_P, ϕ_N, ϕ_S, ϕ_E and ϕ_W. These coefficients represent the influence of the values of the neighboring ϕ s and the source terms on the value of the nodal ϕ value, ϕ_P. The effects of the hybrid differencing scheme are reflected through the values of these coefficients, as they are dependant on the cell Peclet number. The coefficient coupling ϕ_P with ϕ_E, for example, is written as

$$a_E = \begin{cases} \frac{\Gamma_e A_e}{\delta x_e} - \frac{1}{2}\rho u_e A_e & \text{for } |Pe| \leq 2 \\ 0 & \text{for } Pe > 2 \\ -\rho_e u_e A_e & \text{for } Pe < -2 \end{cases} \tag{10}$$

The other coefficients can be expressed in a similar manner. The details of the derivation of the coefficients and the hybrid differencing scheme can be found in the text by Patankar [95].

$Eq(9)$ is the algebraic equation which links the nodal ϕ value with the values of the neighboring ϕ s. Equations like $eq(9)$ are established for all the nodal points in the domain. The next step is to solve these equations. The solution procedure adopted in SOLID-3 is the Line by Line method which employs the Tri-Diagonal Matrix Algorithm. In this technique the equation set for each row or each column (a line) of grid nodes is set up, assuming the ϕ s in the neighboring lines to be known. This results in a tri-diagonal equation set for each line, which can be solved very efficiently. The solution then proceeds on to the next line and in this manner the entire computational domain is swept in a line by line fashion.

3.3 Boundary Conditions

The application of the boundary conditions is simple for rectangular domains. Fig. 2 shows a non-uniform grid specified in a rectangular domain. Insertion of the

boundary conditions requires modification of the finite difference formulation for nodes adjacent to those at the boundaries.

The first step in the application of the boundary conditions is to break the nodal coupling by setting the appropriate coefficients (a_N, a_S, a_E or a_W) to zero. The boundary condition is then imposed by modifying the source terms in the algebraic equations for the near boundary nodes. The following types of boundary conditions can be imposed:

3.3.1 *Fixed Heat Flux*

Suppose that the value "H" has to be specified for the diffusion heat flux $\Gamma_h \frac{\partial h}{\partial y}$ at the north boundary of the domain. In this case the source terms for the nodes at the row "NJ-1" have to be redefined during the solution of the energy equation as

$$Su = Su - \frac{HA_n}{V} \tag{11}$$

$$Sp = 0 \tag{12}$$

where "A_n" is the area of the north wall of the cell and "V" is the cell volume. If "H" is zero than the north boundary becomes adiabatic.

3.3.2 *Fixed Temperature*

If a value "T_f" is specified for the temperature (or "h_f" for the sensible enthalpy) at the north boundary of the domain then for the cells at the "NJ-1" row the source terms have to be modified as follows

$$Su = \Gamma_h \frac{A_n}{\delta r} h_f \tag{13}$$

$$Sp = -\Gamma_h \frac{A_n}{\delta r} \tag{14}$$

3.3.3 *Mold Casting Interface*

Heat transfer taking place across the mold casting interface is assumed to consist of conduction at local points of contact, conduction through the air in the gap and radiation between the surfaces of the mold and the casting. Consider the interface cell pair shown in Fig. 3. The heat transfer can be expressed as:

(i) Conduction at local points of contact:

$$\wp(T_c - T_m) \tag{15}$$

where

$$\wp = \frac{gA}{(\Delta x_m/k_m + \Delta x_c/k_c + R)} \tag{16}$$

(ii) Conduction through the air in the interfacial gap:

$$\xi(T_c - T_m) \tag{17}$$

where

$$\xi = \frac{(1-g)k_a A}{\Delta x} \tag{18}$$

(iii) Radiation across the interfacial gap:

$$\varsigma(T_c - T_m) \tag{19}$$

where

$$\varsigma = (1-g)\sigma\epsilon A[(T_c + 273.15)^2 + (T_m + 273.15)^2]$$
$$[(T_c + 273.15) + (T_m + 273.15)] \tag{20}$$

The implementation of the interface condition is as follows. First the linking coefficients of the mold and casting cells are set to zero. Therefore, for the mold node in Fig. 3 set

$$a_E = 0 \tag{21}$$

and for the casting node set

$$a_W = 0 \tag{22}$$

The interface heat transfer is now imposed through the source terms for the mold nodes as

$$Su = Su + (\wp + \xi + \varsigma) + \frac{h_c}{C_c} \tag{23}$$

$$Sp = Sp - \frac{(\wp + \xi + \varsigma)}{C_m} \tag{24}$$

and for the casting nodes as

$$Su = Su + (\wp + \xi + \varsigma) + \frac{h_m}{C_m} \tag{25}$$

$$Sp = Sp - \frac{(\wp + \xi + \varsigma)}{C_c} \tag{26}$$

where h_c and h_m are the sensible enthalpies of the casting and mold nodes respectively and C_c and C_m are the specific heats of the casting and mold materials.

3.4 Latent Heat of Fusion:

The latent heat release is taken into account by a source based technique originally proposed by Voller et. al. [98,99]. In this work the technique has been extended to handle eutectic materials. A new equation is also derived for the

isothermal solidification stage and it shows better convergence behaviour compared to the equation originally proposed.

The governing differential equation, $eq(1)$, written for $\phi = h$ yields the energy equation, which when discretized by the Finite Volume Method provides the algebraic equation, say for iteration i as

$$a_P h_{P_i} = \sum ah + a_P^o[h_P^o + (H_P^o - H_{P_i})] \tag{27}$$

In the above equation "h" is the nodal sensible enthalpy defined as the product of the nodal specific heat and temperature, "H" is the nodal latent heat content, "a" are the nodal coupling coefficients and "$\sum ah$" is the sum of the products of "a" and "h" for the neighboring cells. During the solidification stage the value of "H_{P_i}" is unknown in $eq(27)$ and a model has to be devised for it's determination.

Cast Iron is a eutectic material, therefore it releases part of it's latent heat between the liquidus and solidus temperatures and part of it's latent heat at the solidus temperature. Let the total heat of fusion of Cast Iron be "L" and the heat of fusion released at the solidus temperature be "L_2". Assuming a linear relation between the temperature (or sensible enthalpy, h) and latent heat release the following relation between sensible enthalpy and nodal latent heat content "H" is obtained.

$$h_{P_i} = \varphi_1 H_{P_i} + \varphi_2 \tag{28}$$

where

$$\varphi_1 = \frac{h_{liq} - h_{sol}}{L - L_2} \tag{29}$$

$$\varphi_2 = h_{liq} - \varphi_1 L \tag{30}$$

Rewriting $eq(27)$ for the $(i-1)$th iteration involves only replacing the subscript i by $(i-1)$

$$a_P h_{P(i-1)} = \sum ah + a_P^o[h_P^o + (H_P^o - H_{P(i-1)})] \tag{31}$$

At the ith iteration the nodal sensible enthalpy has to account for the nodal latent heat, and therefore $eq(28)$ has to be satisfied simultaneously with $eq(27)$. Substituting h_{P_i} from $eq(28)$ into $eq(27)$ and eliminating $\sum ah$ with $eq(31)$ yields

$$H_{P_i} = \frac{1}{a_{P_o} + a_P\varphi_1}(a_{P_o}H_{P(i-1)} + a_P h_{(i-1)} - a_P\varphi_2) \tag{32}$$

The above equation defines H_{P_i} in terms of known previous iteration parameters. This equation is, of course, applicable only between the liquidus and solidus temperatures. In the derivation of this equation the assumption that $\sum ah$ does not change between iterations is implicit. This assumption is true during the iterations approaching final convergence. At the solidification temperature the nodal sensible enthalpy remains constant at h_{sol} while latent heat is being released. Substituting $h_{P_i} = h_{sol}$ in $eq(27)$ and eliminating $\sum ah$ with $eq(31)$ yields

$$H_{P_i} = H_{P(i-1)} + \varsigma\frac{a_P}{a_P{}^o}(h_{(i-1)} - h_{sol}) \tag{33}$$

The above equation defines H_{P_i} in terms of previous iteration parameters for isothermal solidification. The same assumption to eliminate $\sum ah$ has been made as for $eq(32)$. The term ς defines an under relaxation factor (about 0.8) to help convergence.

The latent heat release is therefore taken into account in the solution of $eq(27)$ and the evaluation of H_{P_i} by $eq(32)$ if $h_{sol} < h \leq h_{liq}$ and $eq(33)$ if $h = h_{sol}$.

3.5 Velocity Treatment During Solidification

The natural convection in the liquid metal takes place because of thermal gradients. The Boussinesq approximation is used in which the liquid is treated as incompressible and the density differences are considered only to determine the body forces causing the free convection.

During the simulation of the solidification stage the velocity computations have to be modified to take the freezing of the liquid metal into account. Three different techniques to suppress the velocities during solidification have been incorporated into SOLID-3.

3.5.1 *D'Arcy Source Method*

During the solidification of eutectic metals the formation of dendrites takes place which causes the "mushy" zone to behave as a porous medium. According to D'Arcy's law, the velocity of liquid flowing through porous media is proportional to the pressure gradient.

$$v = -C\eta \frac{\partial p}{\partial x} \tag{34}$$

or

$$\frac{1}{C\eta} v = -\frac{\partial p}{\partial x} \tag{35}$$

where C is a constant and η is the porosity.

The implementation technique for this method is as follows:

The solid fraction of each velocity cell is monitored. As the solid fraction increases, the porosity $\eta \rightarrow 0$ and $\frac{1}{C\eta} \rightarrow \infty$. What is required is a model relating the porosity with the solid fraction. Consider the solid, mushy and liquid zones shown in Fig. 4. In this model the dendrites are assumed to have a triangular shape and extend from the solid to the liquid regions. For this case a linear relationship will

exist between the porosity and the solid fraction. The term $\frac{1}{C\eta}$ can therefore be modelled as :

$$\frac{1}{C\eta} = Bs \tag{15}$$

where "B" is a large constant and "s" is the solid fraction. Hence as the solid fraction increases, $\frac{1}{C\eta}$ will grow to a very large numerical value.

The term $\frac{\partial p}{\partial z}$ is already present in the momentum equation. The term $\frac{1}{C\eta}$ in $eq(35)$ is a factor of the velocity and hence can be incorporated in the "Sp" term as

$$Sp = Sp - |Sp|Bs \tag{37}$$

When the solid fraction is zero, "Sp" will not be modified, however when the solid fraction increases, "Sp" will grow very large and dominate the diagonal term of the equation

$$(a_p - Sp)v = \sum av + Su \tag{38}$$

Hence in the final solution the numerical value of the velocity "v" will be increasingly suppressed through the mushy range until it is negligibly small in the solidified region.

3.5.2 *Fixed Velocity Method*

In this technique zero normal velocities are imposed on the walls of scalar cells which have solidified. The procedure to implement this is as follows:

The solid fraction of the two scalar cells (adjacent to each face on which a velocity is defined) is monitored. If either of these scalar cells solidify completely then the velocity on the face is imposed to zero by setting

$$Su = 0 \tag{39}$$

$$Sp = -10^{30} \tag{40}$$

in the equation for that velocity. For a velocity "v" the equation is written as:

$$(a_p - Sp)v = \sum a_i v_i + Su \tag{41}$$

If either of the neighboring scalar cells "solidify' completely, the numerical value of the velocity "v" will be suppressed close to zero in the solution of the above equation. This method is very simple to implement and is suited to pure materials or eutectic alloys where solidification is isothermal.

3.5.3 *Increased Viscosity Method*

In this method the viscosity of the liquid metal is increased as it's temperature drops. the procedure to implement this is as follows:

Couple the solid fraction of scalar cells to the viscosity of the liquid metal in the cell by the following model:

$$\mu = \mu_{lm} exp(Bs) \tag{42}$$

where "μ_{lm}" is the viscosity of the liquid metal, "B" is a large number and "s" is the solid fraction. As the solid fraction increases the viscosity increases exponentially and the velocities in the solidifying metal gets suppressed.

4 SOFTWARE STRUCTURE

The SOLID-3 computer program has been developed from the University of Ottawa code TEMA [97]. The code has been written in IBM VS-FORTRAN which is essentially FORTRAN-4 with some extensions. The software has been designed with the objective of maximizing simplicity and ease of amendment. This has been achieved by keeping the main program to be very simple and to subdivide the computational task among a number of subroutines. Fig. 5 shows a simplified flowchart. The code is very well commented and easy to follow. Due to the length of the code it is not possible to describe the function of each line, however the functions of many lines and variables are obvious from the overall context and variable names. A list of the major variable names can be found in the Appendix. The tasks of the major subroutines are described in the following sections. In order to obtain the maximum benefit out of the following sections the user is recommended to follow the program description on an actual listing of SOLID-3.

4.1 The MAIN program

The purpose of the MAIN program is to provide the basic problem parameters and then to act as a *maestro* in coordinating the use of the subroutines to perform the computational task.

The program starts by the specification of equation indices and parameters, for example, "GREAT" and "SMALL" which specify computationally large and small limits. The first item of interest to the user is the problem specification where the type of solidification modelling procedure is selected. The variable "DARCY" selects the D'Arcy source solidification method, the variable "VISBIG" selects the increased viscosity method and the variable "VELFIX" selects the Fixed Velocity Method. These are logical variables which can either have a value of "TRUE" or "FALSE". The next line determines if the problem is steady or transient. "STEADY

= .FALSE." results in a transient solution while "STEADY = .TRUE." results in a steady state solution.

Next a call is made to "ENTRY SPECIF" (SUBROUTINE PRODEP) to define body forces, time steps and temperature boundary conditions. After that the problem dimensions and coordinate system is selected by the variables "INDCOS" and "NDIMEN". Next a call is made to "ENTRY COOR" (SUBROUTINE PRODEP) to define "NI", "NJ" and "NK", the limits of the computational domain along the axial, radial and circumferential directions. The next few calls define the geometry of the problem. The user has to be concerned with "ENTRY RGRIDI" (SUBROUTINE PRODEP) where the basic rectangular geometry can be modified and "ENTRY GEOM" (SUBROUTINE PRODEP) where the geometric locations of the grid lines are defined.

The next line of interest is the specification of the variable "MFLOW" which determines if convection is to be computed. " MFLOW=.TRUE." switches on the computation of convection while MFLOW=.FALSE. switches it off and only conduction is computed. The next few lines define some logical variables for calling later subroutines.

In the next line the reference pressure location is defined by the nodal location "IPREF, JPREF, KPREF". If IPREF=999, a reference pressure is not maintained and the pressure field is allowed to float. This option is required in solidification modelling as a reference pressure definition inside the solidified region has no meaning.

In the next line, "MAXIT" sets the upper limit to the number of iterations required for convergence. This should be rarely more than 500 to 800 unless the problem is highly nonlinear and heavy under-relaxation is used. "SORMAX" is the maximum allowable value of the normalized source imbalance permitted at

convergence. This can be usually about 0.1 to 1 percent of some reference field value, depending on how stable the solution is in the iterations preceding the final convergence.

The next few lines define "IMON, JMON and KMON", the nodal coordinates of the field value monitoring location. The field values at this location will be written every second cycle on unit 6 and every "INDPRI" cycle on unit 2.

The next lines define the "URF" array, the under-relaxation factors for the different ϕ's. The next lines define "NSWP", the array specifying how many times the solver has to sweep the domain in order to obtain the maximum benefits from the updated coefficients. The user is advised not to disturb these parameters until he has had fair experience in the operation of the code. After this "PATM" and "PREF" are defined as the atmospheric pressure and the reference pressure respectively. The reference pressure is the pressure maintained at the location "IPREF, JPREF KPREF" if "IPREF" is not equal to 999.

The next few lines define the basic problem parameters and material properties. Each line of this section of the code is commented and therefore does not need additional explanation here.

Next, the arrays are initialized to zero, the domain boundaries are set and the initial and boundary conditions are defined. After that the initial information is written out on the output file and the iteration operations start.

In the transient case the present field values are first stored in core and then the time step is advanced. After that subroutine "CHKSOL" is called to decide if enough cells are in the liquid phase to warrant flow computation. At this time some headings are written on the two output files on unit 2 and unit 6.

The solution iterations now start. First the velocity fields are solved for, then the pressure and velocity corrections are performed. Next some temperature dependant

boundary conditions are computed, for example, viscosity updating (in case the Increased Viscosity Method is used) and computation of the free convection heat transfer coefficients at the mold outer surfaces. In the next steps the residual source values are normalized and written at unit 6 for every even iteration. Next the maximum normalized source is compared against the source limit, SORMAX, and a decision about convergence has to be made. If the residual source is greater than the maximum limit, another iteration is performed. After about 20 iterations if the residual source is too large something is usually wrong and the run is aborted. If the residual source does not reduce within the maximum number of iterations the run is aborted. If the residual sources do reduce below the maximum limit, the solution is considered to be converged, the field residuals are written out if required and the program proceeds on to the next time step solution. This process continues until the maximum time limit is reached or the casting solidifies completely, at which point the run terminates. In the following sections the tasks of the main subroutines are described.

4.2 Subroutine PRODEP

This is the PROblem-DEPendant subroutine where modifications are made to the standard program configuration. It contains many different sections; each section has it's own ENTRY and therefore can be called separately. These sections are discussed in the following:

4.2.1 *ENTRY SPECIF*

In this section the basic problem parameters are defined. First, the radius and height of the domain is defined. "GACCX", "GACCY" and "GACCZ" define the body forces (accelerations of the coordinate systems) along the three coordinate directions. Next, for steady state solutions the variables for time, time step and time to print are set to zero. After that the boundary conditions for the

velocities and temperatures are set. A wall condition of "TRUE", for example, "WALLE=.TRUE." means a no slip boundary condition, while a wall condition of "FALSE", for example, "WALLS=.FALSE." means a free slip boundary condition. A temperature condition of "TFIXE=.TRUE." means the temperatures at the east boundary will remain fixed, while "TFIXE=.FALSE." means that the heat flux at the east boundary is fixed. For the transient data, "TMAX" is the maximum time for which the simulation is required, "TSTEP" is the time step and "TPRT" is the time step after which output is required.

4.2.2 *ENTRY COOR*

The limits of the grid indices are defined. "NI" is the number of nodes along the x (or axial) direction, "NJ" are the number of nodes along the y (or radial) direction and "NK" is the number of nodes along the circumferential direction. "IFAC1" is the node number for the west face of the mold, "IFAC2" is the node number for the east face of the mold and "JFAC" is the node number for the north face of the mold.

4.2.3 *ENTRY RGRIDI*

If the basic rectangular coordinate system has to be modified, then the modifications are done in this section.

4.2.4 *ENTRY GEOM*

The geometry of the domain is defined here. The array "XU" contains the x coordinates of the vertical grid lines on which "u" velocities are defined, the array "YV" contains the y (or r) coordinates of the horizontal grid lines where "v" velocities are defined and the array "ZW" contains the angle (in radians) of the radial lines where the velocity "w" is defined (in a cylindrical system).

4.2.5 *ENTRY INIT0*

The initial temperature and enthalpy distribution is imposed on the domain.

4.2.6 *ENTRY BOUND0*

The boundary conditions can be imposed here. Also the source normalizing factors, "SNORM", are calculated here. What is required is a typical area "AREAT", a typical velocity, "UIN" and a typical enthalpy, "HREF". These values will be used to normalize the source terms.

4.2.7 *ENTRY INPTD*

The time dependant boundary conditions are set here.

4.2.8 *ENTRY OUTPTD*

This section is for time dependant output calculation.

4.3 Subroutine LATENT

Computations related to the latent heat are performed in this subroutine.

4.3.1 *ENTRY CHKSOL*

This section verifies if there are enough cells in the liquid phase to warrant fluid flow computation. A liquid cell grid of a minimum of 4 by 4 cells is needed.

4.3.2 *ENTRY UPLAT*

This section is computes the solid fraction of the complete computational domain. If the entire domain has solidified, it sets the variable "FROZEN" to "TRUE" which later terminates the computations.

4.3.3 *ENTRY CALDHP*

This sections computes the term ΔH_p to determine the latent heat content at each time step.

4.4 Subroutine PROMOD

This is the PROblem MODification subroutine where boundary conditions are imposed.

4.4.1 *ENTRY FRECON*

In this section the free convection heat transfer coefficients at the mold external surfaces are computed.

4.4.2 *ENTRY MODPRO*

Shear stress coefficients are calculated at the boundaries of the fluid flow computational domain.

4.4.3 *ENTRY ULOWER and ENTRY VLOWER*

Coupling coefficients are set to zero at the boundaries of the fluid flow computational domain.

4.4.4 *ENTRY MODU and ENTRY MODV*

The boundary conditions (free slip or no slip) for the velocities are applied through the modification of the source terms.

4.4.5 *ENTRY UFIX0 and ENTRY VFIX0*

Zero velocities are imposed through the source terms in the cells which have solidified. This section is used if the Fixed Velocity Method is selected for solidification modelling.

4.4.6 *ENTRY UDAR0 and ENTRY VDAR0*

This section is used if the D'Arcy Source Method is selected for solidification modelling. It inhibits the velocities linearly with the increase of the solid fraction.

4.4.7 *ENTRY MODP*

The coupling coefficients are set to zero at the boundaries for the pressure correction equation. The pressure field is imposed through the reference pressure, "PREF" (in the main program) at the point "IPREF, JPREF, KPREF".

4.5 Subroutine MODPHI

This subroutine imposes the boundary conditions for the scalar transport equation.

4.5.1 *ENTRY FILOW*

The coupling coefficients at the near boundary cells are set to zero along the nearest grid line inside the domain.

4.5.2 *ENTRY MODFI*

The boundary conditions are imposed through the source terms in this section.

4.6 Subroutine INIT

4.6.1 *ENTRY GRIDI*

The computational grid boundaries are defined in this section.

4.6.2 *ENTRY GRIDP*

The grid point positions and certain geometrical parameters, such as distances between cells are computed and stored for later use.

4.6.3 *ENTRY GRIDV*

The domain boundaries are redefined for the computation of velocities after the computation of temperatures. This is because the velocities are only computed in the casting region.

4.6.4 *ENTRY GRIDT*

The domain boundaries are redefined for the computation of temperatures after the computation of velocities. This is because the temperatures are computed in the casting and the mold region.

4.6.5 *ENTRY SET*

The variable arrays are initialized in this section.

4.6.6 *ENTRY SETSTR*

Shear stress terms are calculated for the boundaries of the casting domain.

4.7 Subroutine PRINT

This subroutine writes out the program output on unit 2.

4.8 Subroutine LISOLV

This subroutine incorporates the TDMA solver which solves the algebraic equations along each grid line. The entire domain is swept along the north-south, east-west and front-back directions in a line by line fashion every time this subroutine is called.

4.9 Subroutines CALCU, CALCV and CALCFI

These three subroutines calculate the velocity and the temperature fields. They have basically the same structure. First the convective and diffusive components are calculated and the nodal coupling coefficients are assembled from them. Second, the boundary conditions are imposed by setting the appropriate coefficients to zero and modifying the source terms. Third, the final coefficient assembly is performed and finally the equation set is solved by calling LISOLV.

4.10 Subroutine CALCP

This subroutine solves the pressure correction equation to obtain the pressure and velocity corrections. First, the coefficients and source terms of the finite volume equations are calculated, then these equations are solved after application of the boundary treatment. After that the pressure and velocity correction are computed and applied.

4.11 Subroutine HYBRID

This subroutine uses the Hybrid Differencing (Upwind/Central) scheme to calculate the nodal coupling coefficients of the finite volume equations.

4.12 Subroutine CORESI

This subroutine performs the final coefficient assembly and incorporates the under-relaxation. It also calculates the total residual source calculation from the previous iteration solution, which is a measure of the degree of convergence of the solution.

4.13 Subroutine ERROR

This subroutine is useful in debugging the code. It is used in writing out field values, coefficients, properties etc on unit 2 for debugging purposes. It can be called from strategic locations in the program to investigate the behavior of the variable fields for error tracing.

4.14 Subroutines PREAD and PWRITE

These are pseudo read-write subroutines to store the previous time step data in core for virtual memory environments. These subroutines greatly improve the speed of the program. There is a provision to store previous time step data on disk for systems which have memory limitations, for example CDC Cyber computers. This is activated by simply commenting out the CALLs to these routines and removing the commenting character "C" from the "READ(10)", "WRITE(10)" and "REWIND(10)" statements preceding the CALLs to subroutines "PREAD" and "PWRITE". Unit 10 is then defined as a scratch file for temporary storage of previous time step data.

4.15 Subroutine SOZONE

This subroutine rezones the liquid computational domain after every time step. This is required to keep the number of "solidified" cells small as compared with the number of cells in the liquid region. If the number of cells in the solid region gets too large as compared to the number of cells in the liquid region, the solution gets prone to numerical instability.

4.16 Subroutine INCO

This subroutine calculates the natural convection heat transfer coefficients at the mold outer surfaces. These coefficients have to be recomputed at each time step as they are coupled to the mold wall temperature.

5 SOLUTION OF A TEST CASE

The test problem to be considered is the solidification of a cylindrical grey iron casting in a permanent mold. A schematic diagram of the mold and casting is shown in Fig. 6(a). The mold consists of a cast iron cylinder of 0.05 m thickness. A 0.05 m thick cast iron cover plate forms the upper part of the mold. The mold is placed on a 0.4 m thick sand base with a gating system to allow the liquid metal to enter the mold cavity axially at the center.

5.1 Problem Assumptions and Boundary Conditions

The mesh used is shown in Fig. 6(b). The solution of the problem is based on the following assumptions:

1) Convection in the liquid metal due to pouring is negligible.
2) The pouring time of the casting is negligible as compared with the total solidification time.
3) The flow of the liquid metal due to natural convection is laminar.
4) Initially, the heat transfer between the casting and the mold is due to conduction through a mold-casting thermal contact resistance.
5) A gap forms at the mold-casting interface after the first layer of casting cells neighboring the interface solidify completely. After gap formation, the heat transfer across the gap is due to radiation between the casting and mold surfaces and conduction through the air in the gap.
6) Cast Iron is a eutectic; it releases part of it's latent heat as it cools from the liquidus to the solidus temperature and the rest of the latent heat at the solidus temperature.
7) The heat transfer from the mold outside surface occurs through free convection to the ambient air.

The initial conditions (due to assumptions (1) and (2)) are:

MEDIUM	ϕ	RANGE
Cast Iron	$T = T_{pour}$	$o \leq r < b$
(Casting)	$u = 0,\ v = 0$	$d < x < f$
Cast Iron	$T = T_{mold}$	$b \leq r \leq c$
(Mold)		$d \leq x \leq f$
Cast Iron	$T = T_{mold}$	$o \leq r \leq c$
(Cover)		$f \leq x \leq g$
Sand	$T = T_{mold}$	$o \leq r \leq c$
(Mold Base)		$o \leq x \leq d$

The boundary conditions are:

(a) Temperature:

The conditions at the boundaries for the computational domain of the energy equation are:

Top Surface of Mold:

$$-k\frac{\partial T}{\partial x}|_{x=g} = F_t(T_t - T_{amb})$$

Side Surface of Mold:

$$-k\frac{\partial T}{\partial r}|_{r=c} = F_s(T_s - T_{amb})$$

Bottom Surface of Mold:

$$-k\frac{\partial T}{\partial x}|_{x=o} = 0$$

Centerline (Axis of symmetry):

$$-k\frac{\partial T}{\partial r}|_{r=o} = 0$$

where the subscripts t, s, b and o denote the top, side and bottom surfaces and the axis of symmetry respectively. The symbol F represents the free convection heat transfer coefficients at the mold boundaries.

The boundary conditions at the mold casting interface are specified as follows:

(Before gap formation):

$$-k_{eff,casting}\frac{\partial T}{\partial r}|_{r=ca} = -k_{eff,mold}\frac{\partial T}{\partial r}|_{r=mo}$$

(After gap formation):

$$-k_{casting}\frac{\partial T}{\partial r}|_{r=a} = h^*(T_a - T_b) + \epsilon\sigma_b(T_a^4 - T_b^4)$$

where the subscript eff means the effective values of conductivity which take the thermal contact resistances into account. The subscripts mo and ca represent the mold and casting surfaces in contact. Similar equations can be written for the horizontal interfaces.

(b) Velocity:

The boundary conditions for the solution of the momentum equations are as follows:

$u = 0,\ \frac{\partial v}{\partial r} = 0 \qquad r = b$

$\qquad\qquad\qquad\qquad d < x < e$

$v = 0,\ \frac{\partial u}{\partial x} = 0 \qquad x = d$

$\qquad\qquad\qquad\qquad o < r < b$

$$v = 0,\ \frac{\partial u}{\partial x} = 0 \qquad x = f$$
$$o < r < b$$

5.2 Results and Discussion

In this study the effects of pouring have been neglected and the computations are started by the assumption of a uniform temperature and zero velocity field. Fig. 7 shows the velocity and temperature fields at time = 50 seconds.

The solid line shows the solidus interface. The maximum Raleigh number for this problem is about 2×10^6 so the free convection is in the laminar range. The liquid metal near the solidus interface cools down and flows to the bottom of the mold cavity while the relatively hotter metal in the center rises towards the top. The maximum velocity is about 3 mm/s. It can be seen that the relatively colder liquid metal that is falling parallel to the solidus interface reduces the temperatures in the lower half of the casting. This causes the solidification to proceed somewhat faster in the bottom region and raises the level of the point where solidification occurs last as compared with pure conduction results. In the present study the rise of this level was about 0.6 cm in a 10 cm casting, or about 6%. The accurate prediction of the location to solidify last is important because this location usually contains porosity and shrinkage defects. The relatively hot metal which rises in the center and then flows towards the interface causes the hottest location in the casting to move radially outward from the center. This location moves back to the center at the later stages of solidification, when the liquid metal convection currents die out.

Fig. 8 shows the computed temperature profiles along the horizontal midsection of the casting. The results shown are for runs in which: (1) Only conduction was simulated, (2) Solidification was simulated by the D'Arcy Source method, (3) Solid-

ification was simulated by imposing zero velocities in the solidified cells. Method (2) is applicable to materials which solidify over a liquidus-solidus range while method (3) is suited for pure materials which solidify isothermally. It can be seen that the liquid metal flow has the effect of flattening out the temperature profile. This effect is more pronounced for method (3) than for method (2), the reason being that in the latter the resistance to the flow due to the dendrites is taken into account, and this has the effect of reducing the velocities.

Fig. 9 shows the temperatures at two monitoring locations (*i*), (*ii*) at the center of the casting for the three methods discussed in the previous paragraph. It can be seen that including the effects of the fluid flow in the heat transfer computations causes the temperatures at the center of the casting to drop sooner. If the D'Arcy approach, method (2), is used then the effects of the velocity field are negligible after about 120 *s*. If cast iron were a "pure" material then method (3) would be applicable. In that case it can be seen that not only would the temperatures be significantly lower but solidification would also occur much earlier. The total solidification times were 285 *s* for method (1), 280 *s* for method (2) and 255 *s* for method (3). Liquid metal flow enhances heat transfer and the more vigorous the flow, the faster the solidification. This can also be seen from Fig. 10, which shows the heat transfer coefficients at the top and side interfaces. Essentially no difference in the interface heat transfer was found for conduction and conduction/convection results if the mushy range was simulated by the D'Arcy method. The liquid metal flow is more vigorous if effects of the dendrites are not modelled (method (3)) and the heat transfer coefficients are larger. This effect is more pronounced at the top interface because the casting temperatures are higher (due to the rising of the hotter liquid metal at the center) and therefore the radiative component for the heat transfer coefficient is larger. The sharp drop for the side interface value at about

40 *secs* is due to gap formation after the outermost layer of casting cells solidifies. It can be seen that for method (3) the gap formation time is larger, as the outer layer of the casting cells took longer to solidify.

5.3 CONCLUSIONS

The heat transfer due to free convection may be less significant than the conductive heat transfer in metals which exhibit a large mushy zone. Convection is geometry dependant, therefore general conclusions about it's importance cannot be made before the actual computations are carried out. Another very important parameter is the resistance that the dendrites provide to the flow of the liquid metal. It is possible that there may not be a linear relation between the solid fraction and the resistance to flow, as assumed in this study. In that case the effects of the flow would be larger than predicted by the linear implementation of the D'Arcy model. The validity of this model should be verified by experimental data on porosity.

Even if the convective heat transfer is negligible, the computation of liquid metal flow in the mushy region is required for the calculation of segregation. The model developed in this paper can be very useful for this application.

The liquid metal flow calculations are very important for modelling solidification of pure materials or alloys of eutectic composition. In those cases a mushy zone does not exist and as demonstrated by this study, the convective heat transfer can be very important.

The fluid flow computations during the filling of the mold will be essential for providing the correct initial conditions for the solidification stage. This would be required for both mushy or isothermal solidification cases. For these reasons it is concluded that efforts to simulate fluid flow during casting processes should continue.

REFERENCES

1 Reade, J., Canadian Foundry Association, Personal communications, Ottawa, Ontario

2 Ellis, W. R. "An Inventory of the Canadian Ferrous Foundry Capabilities". Report produced by the Resource Industries Branch, Department of Industry, Trade and Commerce, Federal Government of Canada. Ottawa, Ontario. 1982.

3 Lazardis, A. "A Numerical Solution of the Multidimensional Solidification (or Melting) Problem ", Int. J. Heat Mass Transfer, V. 13, pp. 1459-1477, 1970.

4 Lazardis, A. "A Computer Aided Solution of the Solidification Problem ", AFS Cast Metals Research Journal, March 1974.

5 Pehlke, R. D., Kirt, M. J., Marrone, R. E., Cook, D. J. " Numerical Simulation of Casting Solidification ", AFS Cast Metals Research Journal, V. 9, No. 2, June 1973, pp. 49-55.

6 Jeyarajan, A., Pehlke, R. D. "Numerical Simulation of Casting Solidification", AFS Transactions, V. 9, No. 2, June 1973, pp. 457-464.

7 Davies, V. L. "Feeding Range Determination by Numerically Computed Heat Distribution". AFS Cast Metals Research Journal, June 1975, pp. 33-44.

8 Reddy, G. P. "Design at the External Corners of V Junctions Using Numerical Techniques ", AFS Transactions V. 85, 1977, pp. 597-608.

9 Brody, H. D., Stoehr, R. A. " Computer Simulation of Heat Flow in Casting", Journal of Metals, September 1980, pp. 20-27.

10 Stoehr, R. A. "Simulations in the Designs of Sand Castings", Proceedings of the conference on Modelling of Casting and Welding Processes, The Met. Soc. of AMIE, 1981.

11 Clyne, T. W. "The Use of Heat Flow Modelling to Explore Solidification Phe-

nomena", Metallurgical Transactions B, V. 13B, September 1982, pp. 471-478.

12 Ohtsuka, K., Mizuno, K., Yamada, J. "Application of a Compute Simulation System to Aluminum Permanent Mold Castings", AFS Transactions, V. 90, 1982.

13 Zeng, X. C., Pehlke, R. D. "Numerical Simulation of Solidification For a Copper-Base Alloy Casting", AFS Transactions, V. 92, 1984, pp. 479-488,

14 Marrone, R., E., Wilkes, J., O., Pehlke, R. D. "Numerical Simulation of Solidification, Part I: Low Carbon Steel Casting - 'T' Shape", AFS Cast Metals Research Journal, Dec. 1970.

15 Marrone, R., E., Wilkes, J., O., Pehlke, R. D. "Numerical Simulation of Solidification, Part II: Low Carbon Steel Casting - 'L' Shape", AFS Cast Metals Research Journal, Dec 1970.

16 Jeyarajan, A., Pehlke, R. D. "Casting Design by Computer" AFS Transactions, V. 83, 1975, pp. 405-412.

17 Low, C. H. S. "Fluid Flow During Argon-Stirring in Ladles and Heat Transfer During Solidification in Molds", MASc. Thesis., Mechanical Engineering, University of Ottawa, 1982.

18 Weatherwax, R. B., Riegger, O. K. "Computer Aided Solidification Study of a Die-Cast Aluminum Piston" AFS Transactions, V. 85, 1977, pp. 317-322.

19 Abis, S. " Numerical Simulation of Solidification in an Aluminum Casting ", Metallurgical Transactions B, V. 17B, March 1986, pp. 209-216.

20 Hong, C. P., Umeda, T., Kimura, Y. " Numerical Models for Casting Solidification: part II. Application of the Boundary Element Method to Solidification Problems ", Metallurgical Transactions B, V. 15B, March 1984, pp. 101-107.

21 Hong, C. P., Umeda, T., Kimura, Y. " Application of the Boundary Element Method to Casting Solidifcation ", Metallurgical Transactions B, V. 15B, March

1984, pp. 101-107.

22 Abdullah, Z., Salcudean, M., Davis, K. "Modelling The Solidification of Cast Iron in Permanent Molds", Proceedings of the Symposium on Computer Modelling of Fabrication Processes and Constitutive Behaviour of Metals, (in Print), Held on May 15-16, 1986. Organized by CANMET/PMRL, EMR, AMCA. Ottawa, Canada.

23 Kublbeck, K., Merker, G. P., Straub, J. "Advanced Numerical Computation of Two Dimensional Time Dependant Free Convection in Cavities ", Int. J. Heat Mass Transfer, V. 23, pp. 203-217.

24 Salcudean, M., Abdullah, Z. " Numerical Simulation of Casting Processes", Paper to be presented at the Eighth International Heat Transfer Conference, San Francisco, USA, August 17-22, 1986.

25 Chvorinov, N. "Theory of the Solidification of Castings" Giesserei, V. 27, 1940, pp. 177-186.

26 Heine, R. W. "Feeding Paths for Risering Castings", AFS Transactions, V. 76, 1968, pp. 463-469.

27 Mertz, J. M., Heine, R. W. " Effect of Casting Geometry on Feeding Distance in White Iron", AFS Transactions, V. 80, 1972, pp. 307-310.

28 Mertz, J. M., Heine, R. W. "Design of T-Junctions in Malleable Iron ", AFS Transactions, V. 80, 1972, pp. 307-310.

29 Loper, C. R., Kotschi, R. M. "Design of Bosses and L Sections for Casting ", AFS Transactions, V. 83, 1975, pp. 173-184.

30 Nehru, K. V. K., Nagarjunasagar, Seshadri, M. R., Ramachandran, E.G. "Prediction of Casting Times in Coated Metallic Molds", AFS Cast Metals Research Journal, V. 11, No. 4, 1975, pp. 113-117.

31 Kotschi, R. M., Loper, C. R. "Effect of Chills and Cores on the Design of

Junctions in Castings", AFS Transactions, V. 84, 1976, pp. 631-640.

32 Kotschi, R. M., Loper, C. R., Frankenburg, R. E., Janowski. L. "Elimination of Shrinkage Defectd Through Casting Redesign", AFS Transactions, V. 85, 1977, pp. 571-576.

33 Kotschi, R. M., Plutshack, L. A. "An Easy and Inexpensive Technique to Study the Solidification of Castings in Three Dimensions", AFS Transactions, V. 89, 1981, pp. 601-610.

34 Kim M. H. " Computer Simulation of Solidification in Simple Shaped Castings", PhD Thesis, Metallurgical Engineering, University of Wisconsin, 1984.

35 Mohan, V., Shenoy, R. N. "Prediction of Solidification Time of Iron Castings in Coated Cast Iron Molds", AFS Transactions, V. 90, 1982

36 Cole, G. S., Bolling, G. F. "Importance of Fluid Flow Motion During Ingot Solidification", AFS Transactions, V. 90, 1982.

37 Ramachandran, N. R., Gupta, J. P., Jaluria, Y. "Thermal and Fluid Flow Effects During Solidification in a Rectangular Enclosure", Int. J. Heat Mass Transfer, V. 25, No. 2, pp. 187-194, 1982.

38 Huang, S. C. "Analytical solution for the bouyancy flow during the melting of a vertical semi-infinite region", Int J. Heat Mass Transfer, V. 28, No. 6, pp. 1231-1233, 1985.

39 Goodling, J. S., Khadar, M. S."One Dimensional Inward Solidification with a Convective Boundary Condition", AFS Cast Metals Research Journal, March 1974.

40 Gau, C., Viskanta, R. " Melting and Solidification of a Melting System in a Rectangular Cavity", International J. Heat and Mass Transfer, V. 27, No. 1, pp. 113-122,1984.

41 Hirt, C.W."Flow Analysis for Non-Experts" Proceedings of the 1983 Engineer-

ing Foundation Conferences "Modelling of Casting and Welding Processes II".

42 Stoehr, R., Hwang, W. S. "Modelling the Flow of Molten Metal having a Free Surface During Entry into Molds", Proceedings of the 1983 Engineering Foundation Conferences, "Modelling of Casting and Welding Processes II".

43 Smith, T. G., Wilkes, J.O. "Laminar Free-Surface Flow into a Vertical Cylinder", Computers and Fluids, V. 3, pp. 51-68, 1975.

44 Sparrow, E. M., Patankar, S. V., Ramadhyani, S."Analysis of Melting in the Presence of Natural Convection in the Melt Region", Transactions of the ASME, V. 99, Nov 1977.

45 Wilkes, J. O. Churchill, S. W. "The Finite Difference Computation of Natural Convection in a Rectangular Enclosure", A.I.Ch.E. Journal, V. 12, No. 1, pp. 161-166, 1977.

46 Peaceman, D. W., Rachford, H. H. "The Numerical Solution of Parabolic and Elliptic Differential Equations", Journal of the Society of Ind. App. Math., V. 3, No. 1, pp. 28-41, 1955.

47 Kee, R. J., McKillop, A.A. "A Numerical Method for Predicting Natural Convection in Horizontal Cylinders with Asymmetric Boundary Conditions", Computers and Fluids, V. 5, pp. 1-14, 1977.

48 Ozoe, H., Mouri, A., Ohmuro, M., Churchill S. W., Lior, N. "Numerical calculations of laminar and turbulent natural convection in water in rectangular channels heated and cooled siothermally on the opposing vertical walls", Int J. Heat Mass Transfer, V. 20, No. 7, pp. 125-137, 1985.

49 Szekely, J., Yadoya, R. T. "The Physical and Mathematical Modelling of the Flow Field in the Mold Region in Continuoue Casting Systems: Part II. The Mathematical Representation of the Turbulent Flow Field", Metallurgical Transactions, V. 4, May 1973, pp. 1379-1388.

50 Kroeger, P. G., Ostrach, S. "The Solution of a Two Dimensional Freezing Problem Including Convection Effects in the Liquid Region", Int J. Heat Mass Transfer, V. 17, pp. 1191-1207, 1974.

51 Guenigault, R., Roots, G. "Effects of Natural Convection on the Inward Solidification of Spheres and Cylinders", Int J. Heat Mass Transfer, V. 28, No. 6, pp. 1229-1231, 1985.

52 Desai, P. V., Kim, C."Heat Losses in Runner Channels" Proceedings of the 1983 Engineering Foundation Conferences "Modelling of Casting and Welding Processes II".

53 Desai, P. V., Berry, J. T., Kim, C."Computer Simulation of Forced and Natural Convection During Filling Of a Casting", AFS Transactions, V. 92, 1984.

54 Stewart, M. J., Weinberg, F. "Fluid Flow Through a Solid Liquid Dendritic Interface", Metallurgical Transactions, V. 3, January 1972, pp. 333-337.

55 Gabathuler, J. P., Weinberg, F. "Fluid Flow into a Dendritic Array under Forced Convection", Metallurgical Transactions B, V. 14B, Dec. 1983, pp. 733-741.

56 Maples, A. L., Poirier, D. R. " Convection in the Two-Phase Zone of Solidifying Alloys", Metallurgical Transactions B, V. 15B, March 1984, pp. 163-172.

57 Gabathuler, J. P., Weinberg, F. "Fluid Flow in a Dendritic Array", Proceedings of the 1983 Engineering Foundation Conferences, "Modelling of Casting and Welding Processes II".

58 Ho, K., Pehlke, R. D. "Mechanisms of Heat Transfer at a Metal-Mold Interface", AFS Transactions, V. 92, 1984, pp. 587-598.

59 Ho, K., Pehlke, R. D. "Transient Methods for Determination of Metal- Mold Interfacial Heat Transfer", Paper presented at the 1983 AFS Casting Congress.

60 Ho., K, Pehlke, R. D. "Transient Methods for Determination of Metal- Mold Interfacial Heat Transfer", AFS Transactions, V. 91, 1983, pp. 689-698.

61 Ho., K, Pehlke, R. D. "Metal Mold Interfacial Heat Transfer", Metallurgical Transactions B, V. 16B, September 1985, pp. 585-594.

62 Sully, L. J. D."The Thermal Interface Between Castings and Chill Molds", AFS Transactions, V. 84, pp. 735-744.

63 Srinivasan, M. N. "Heat Transfer Coefficients at the Casting Mould Interface during Solidification of Flake Graphite Cast Iron in Matallic Moulds", Indian Journal of Technology, V. 20, April 1982, pp. 123-129.

64 Majumdar, J., Raychaudhuri, B. C., Dasgupta, S. "An instrumentation Scheme for Multipoint Measurement of Mould-Metal Gap in an Ingot Casting System", Int J Heat Mass Transfer, V. 24, No. 7, pp. 1089-1095, 1981.

65 Sun, R. C. "Simulation and Study of Surface Conductance for Heat Flow in the Early Stage of Casting", AFS Cast Metals Research Journal, September 1970.

66 Thamban, M. I., Panchanathan, V. "Numerical Simulation of Solidification of Aluminum Alloys in Cast Iron Molds", AFS Transactions, V. 88, 1980, pp. 167-173.

67 Davies, V. L. "Heat transfer in gravity die castings", British Foundrymen Journal, V. 73, 1980, pp. 331-334.

68 Nishada, Y., Matsubara, H. "Effect of pressure on heat transfer at the metal mold inteface", British Foundrymen Journal, V. 69, 1976, pp. 274-278.

69 Yovanovich, M. M. "Thermal contact Correlations", Progress in Astronautics and Aeronautics, V. 83, 1982.

70 Yovanovich, J., DeVaal, Hegazy, A. H. "A Statistical Model to Predict Thermal Gap Conduction Between Conforming Rough Surfaces", Proceedings of the 3rd Joint AIAA/ASME Thermophsics, Fluids, Plasma and Heat Transfer Conference, St. Lois, Missouri, June 7-11, 1982.

71 Yovanovich, Hegazy, A. H. "An Accurate Universal Contact Conductance Corre-

lation for Conforming Rough Surfaces with Different Micro Hardness Profiles", Proceedings of the 18th AIAA Thermophsics Conference, Montreal, June 1-3, 1983.

72 Berry, J. T., Pehlke, R. D. "Computer-Aided Design For Castings", AFS Transactions, (Paper presented at the AFS Conference, Sept. 1980, England) pp. 101-108.

73 Walther, M. K. "Casting Solidification Analysis Using CAST", Modern Casting, March 1984.

74 Erickson, W. C., Houghton, A. V." Simulating the Effect of Thermocouple Assemblies on Temperature Measurements", AFS Transactions, V. 85, 1977, pp. 59-64.

75 Erickson, W. C. "The Use of General Purpose Software in Casting Solidification Simulation", Metallurgical Transactions B, V. 8B, March 1977, pp. 93-97.

76 Erickson, W. C. "Computer Simulation Of Solidification", AFS International Cast Metals Journal, March 1980, pp. 30-41.

77 Grant, J. W. "Thermal Modelling of a Parmanent Mold Casting Cycle", Proceedings of a Symposium sponsored by the Solidification Comittee of the Metallurgical Society of AIME, the Process Modelling Activity of A.S.M. and Engineering, Foundation, New Hampshire, Aug 3-8, 1980. Published by the Metallurgical Society of AIME.

78 Salcudean, M., Abdullah, Z. "CAST-Solidification Modelling Program, Version 1.0", Contract Report submitted with Software to CANMET/PMRL Department of Energy Mines Resources, Government of Canada, September 1985.

79 Salcudean, M., Abdullah, Z. "CAST-Solidification Modelling Program, Version 2.0", Contract Report submitted with Software to CANMET/PMRL Department of Energy Mines Resources, Government of Canada, April 1985.

80 Lunardini, V. J. "Heat Transfer in Cold Climates", Van Nostrand Reinhold Co, Toronto, 1981.

81 Goodrich, L. E. "Efficient Numerical Technoque for one Dimensional thermal Problems with Phase Change", Int. J. Heat, Mass Transfer, V. 21, pp. 615-621, 1978.

82 Morgan, K., Lewis, W. R., Zienkiewicz, O.C. "An Improved Algorithm For Heat Conduction Problems With Phase Change", Civil Engineering Department, University College of Swansea, Singleton Park, Swansea, Wales, U.K.

83 Comini, G., Guidice, S. D. "Finite Element Solution of Non-Linear Heat Conduction Problems with Special Reference to Phase Change ", IJNME, V. 8, pp. 613-624, 1974.

84 Pham, Q. T. "A Fast unconditionally stable finite difference scheme for heat conduction with phase change", Int. J. Heat Mass Transfer, V. 28, No. 11, pp. 2079-2084, 1985.

85 Koler, A.I., Thomas, J.D., Tzavaras, A.A. "Computations of Heat of Fusion in a Mathematical Model for Large Steel Cast Shapes", Cast Metals Research Journal, Dec., 1973.

86 Salcudean, M., Abdullah, Z., Low, C. H., Davis K. "Computation of Heat Transfer in a Casting", Proceedings of the Tenth IASTD International Symposium, Applied Simulation and Modelling, San Francisco, USA, June 4-6, 1984.

87 Zienkiewicz, O.C., Parekh, C.J., Wills, A.J. " The Application of Finite Elements to Heat Conduction Problems Involving Latent Heat", Rock Mechanics, V. 5, No. 76, 1973.

88 Solomon, A.D."A Numerical Study of the Performance of Latent Heat Storage for Solar Dynamic Power Systems", ORNL-6218.

89 Bell, G. E., Wood, A. S."On The Performance of the Enthalpy Method in the

Region of a Singularity", IJNME, V. 19, 1983.

90 Wood, A. S., Richie, S.I.M., Bell, G.,E., "An Efficient Implimentation of the Enthalpy Method", IJNME, V. 17, 1981.

91 Tackle, K. H. "Discretization of the Explicit Enthalpy Mehtod For Planer Phase Change", IJNME, V. 21, 1985.

92 Shamsundar, N., Sparrow, E. M. "Analysis of Multidimensional Conduction Phase Change Via the Enthalpy Model", Transactions of ASME J. Heat Transfer August, 1975.

93 Voller, V., Cross, M."Accurate Solutions of Moving Boundry Problems Using the Enthalpy Method", Int. J. Heat Mass Transfer, V. 24, 1980.

94 Angus, H. T."Cast Iron: Physical and Engineering Properties", 2nd Ed, Butterworths, London, 1976.

95 Patankar, S. V., "Numerical Heat Transfer and Fluid Flow", McGraw-Hill Book Co., 1980.

96 Poirier, D., Salcudean, M. "On Numerical Methods used in Mathematical Modeling of Phase Change in Liquid Metals". ASME Paper 86-WA/HT-22.

97 Lai, M., Salcudean, M., Personal communications and internal University of Ottawa reports.

98 Voller, V. R., Cross, M., Markatos, N., C. " An Enthalpy Method for Convective Diffusive Phase Change" Int. Journal of Numerical Methods in Engineering, 1986.

99 Voller, V. R., Markatos, N., C., Cross, M. " Techniques for Accounting for the Moving Interface in Convection Diffusion Phase Change" Proceedings of the Fourth International Conference on Numerical Methods in Thermal Problems held in Swansea, U. K. July 15-18, 1985.

100 Harlow, F., Amsden, A. "A Numerical Fluid Dynamics Calculation Method for

All Flow Speeds", Journal of Computational Physics, V. 8, pp. 197-213, 1971.

101 Pracht, W. "Calculating Three Dimensional Fluid Flows at All Speeds with an Eularian Lagrangian Computing Mesh" Journal of Computational Physics, V. 17, pp. 132-159, 1975.

102 Chan, R. "A Genralized Arbitrary Lagrangian Eularian Method for Incompressible Flows with Sharp Interfaces" Journal of Computational Physics, V. 17, pp. 311-331, 1975.

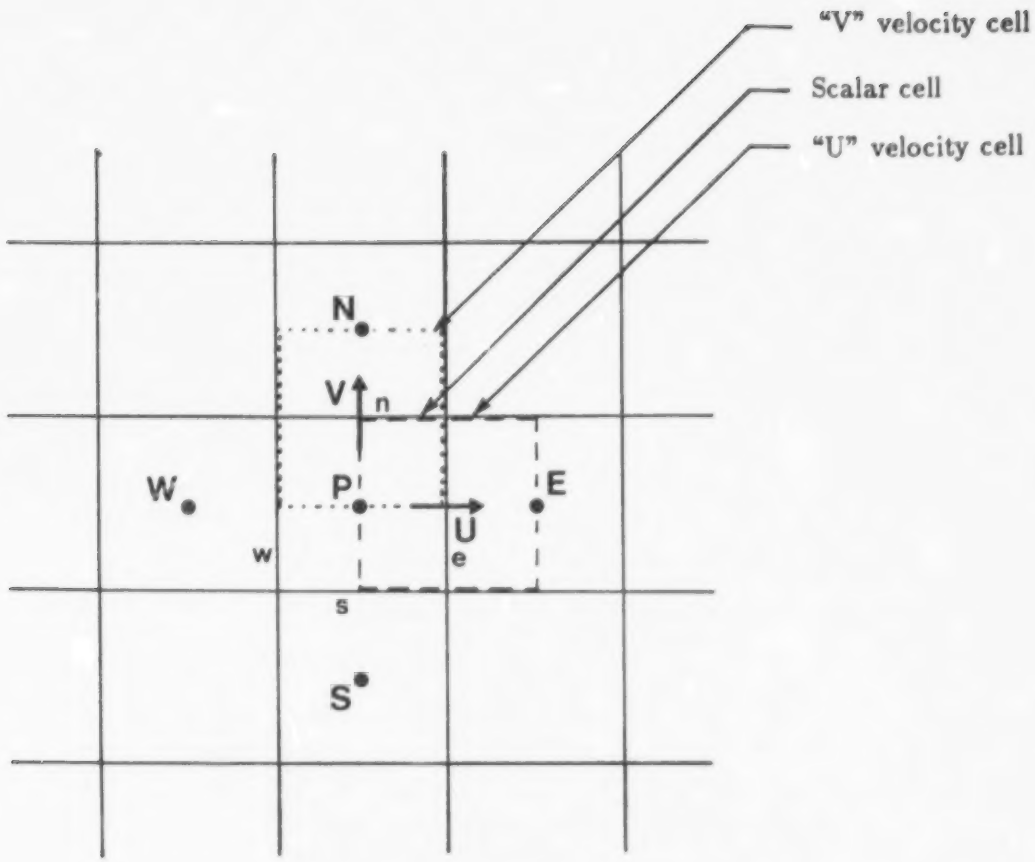

Figure 1 Grid arrangement for the Finite Volume Method

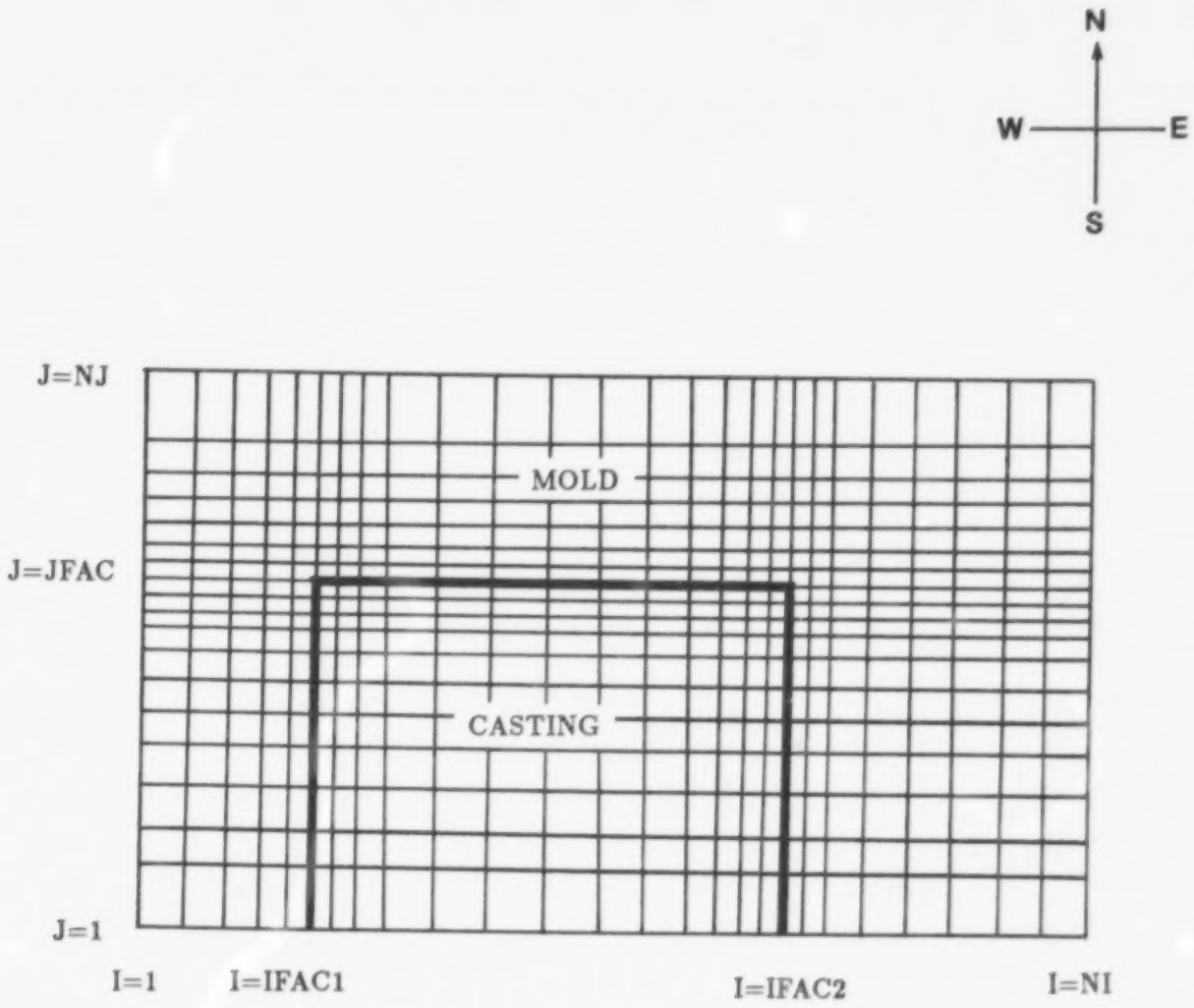

Figure 2 Non-uniform grid specified on a rectangular domain

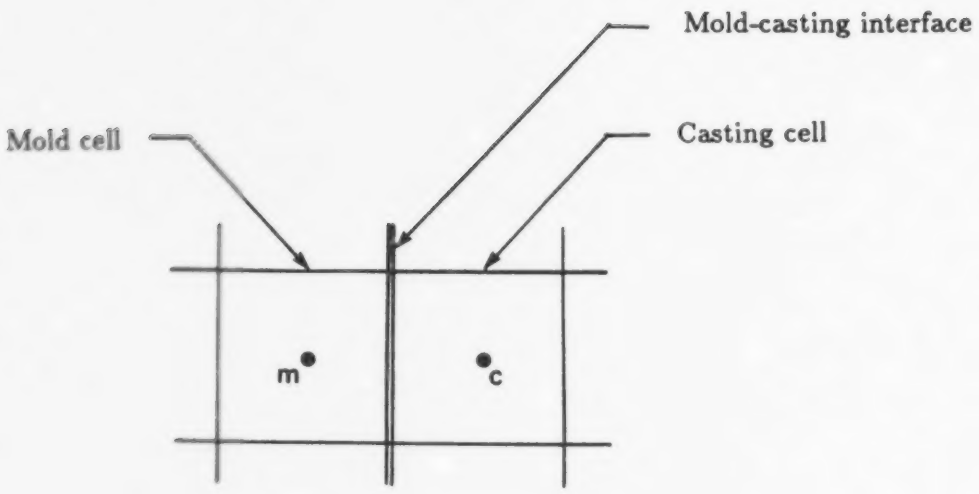

Figure 3 Grid cells at the mold casting interface

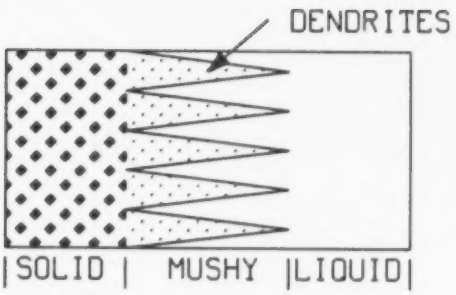

Figure 4 Solid, mushy and liquid zones

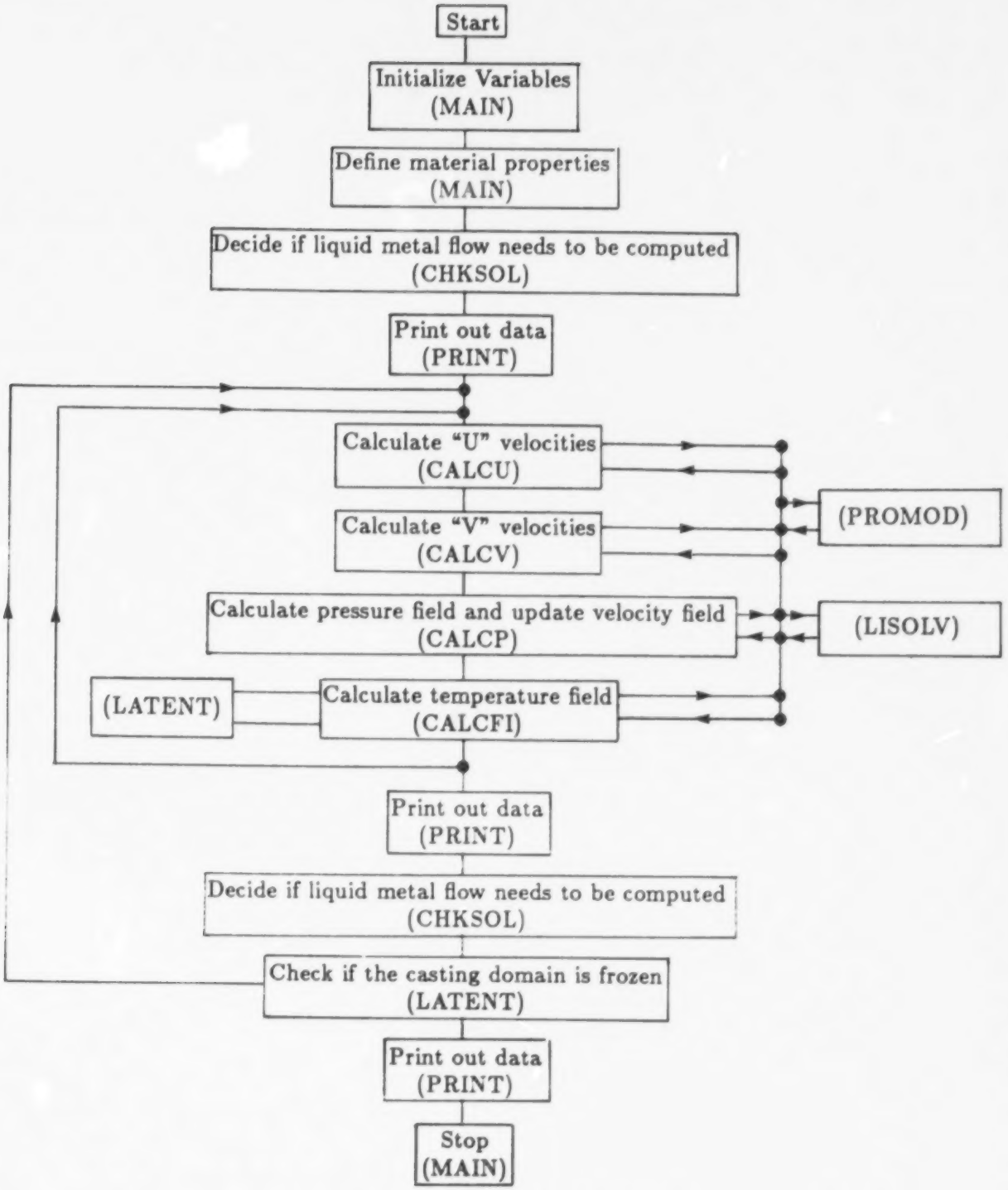
Start
Initialize Variables (MAIN)
Define material properties (MAIN)
Decide if liquid metal flow needs to be computed (CHKSOL)
Print out data (PRINT)
Calculate "U" velocities (CALCU)
Calculate "V" velocities (CALCV)
(PROMOD)
Calculate pressure field and update velocity field (CALCP)
(LISOLV)
(LATENT)
Calculate temperature field (CALCFI)
Print out data (PRINT)
Decide if liquid metal flow needs to be computed (CHKSOL)
Check if the casting domain is frozen (LATENT)
Print out data (PRINT)
Stop (MAIN)

Figure 5 Simplified flowchart of SOLID-3

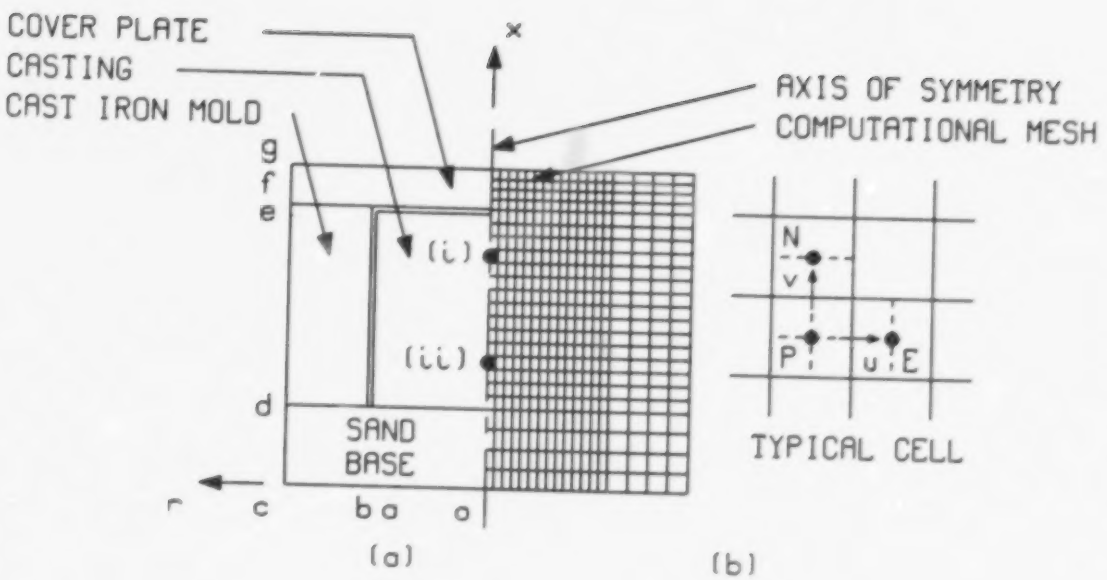

Figure 6 Schematic of the mold and mesh used

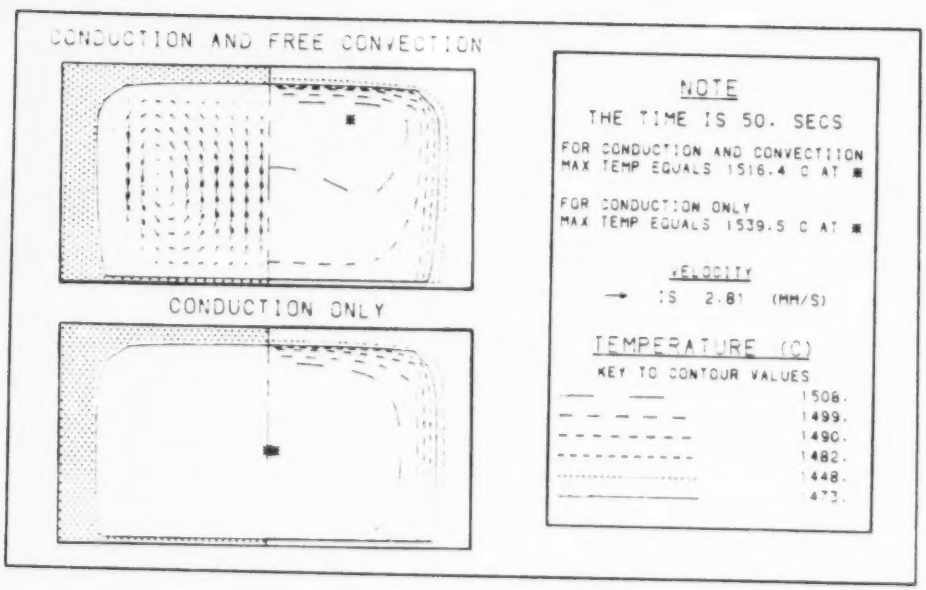

Figure 7 Thermal contours and velocity field in the casting

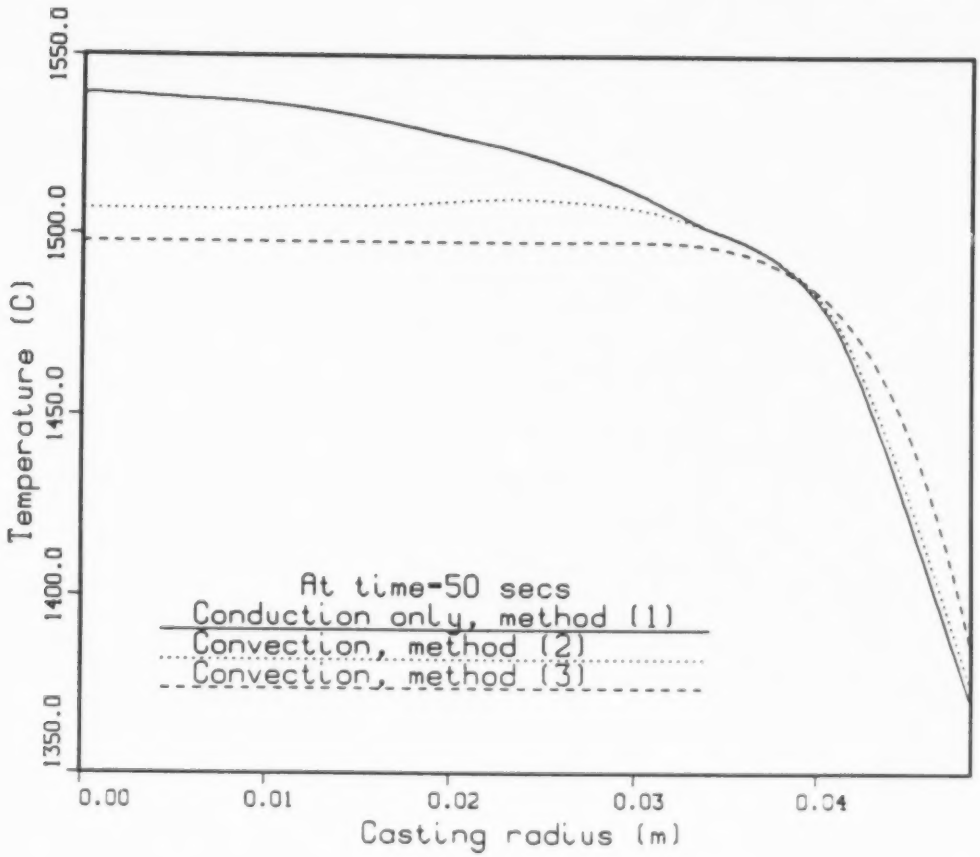

Figure 8 Temperatures at casting midsection

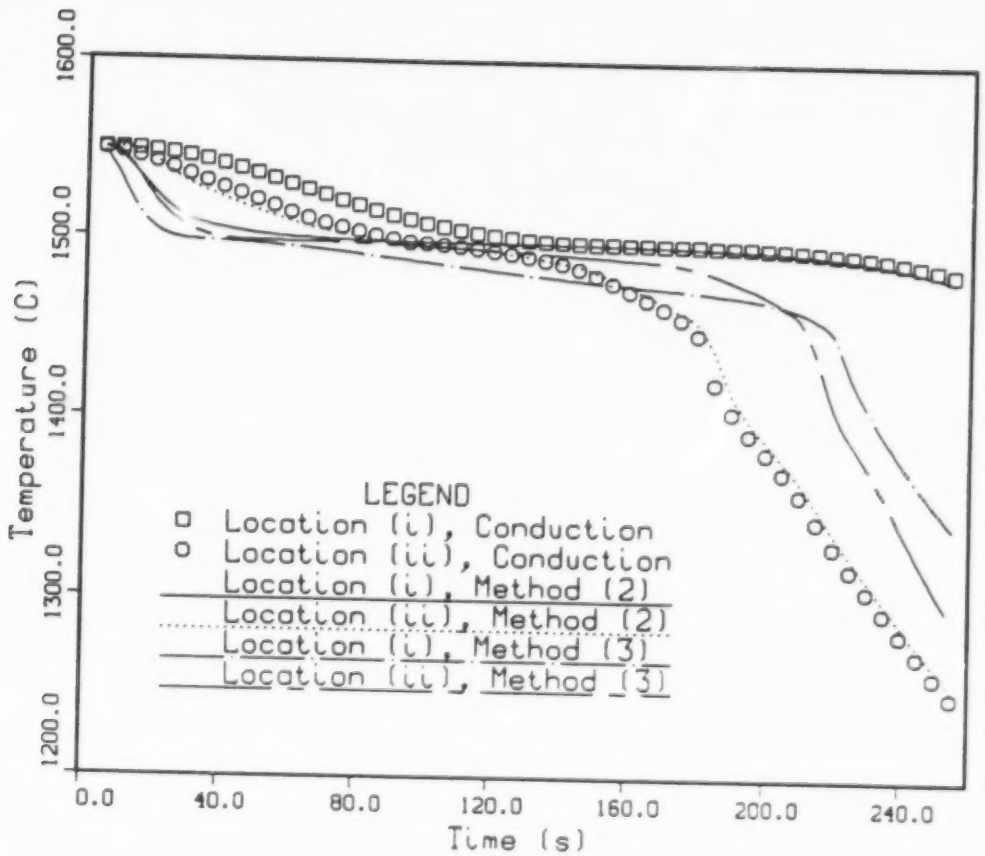

Figure 9 Temperatures at casting centerline

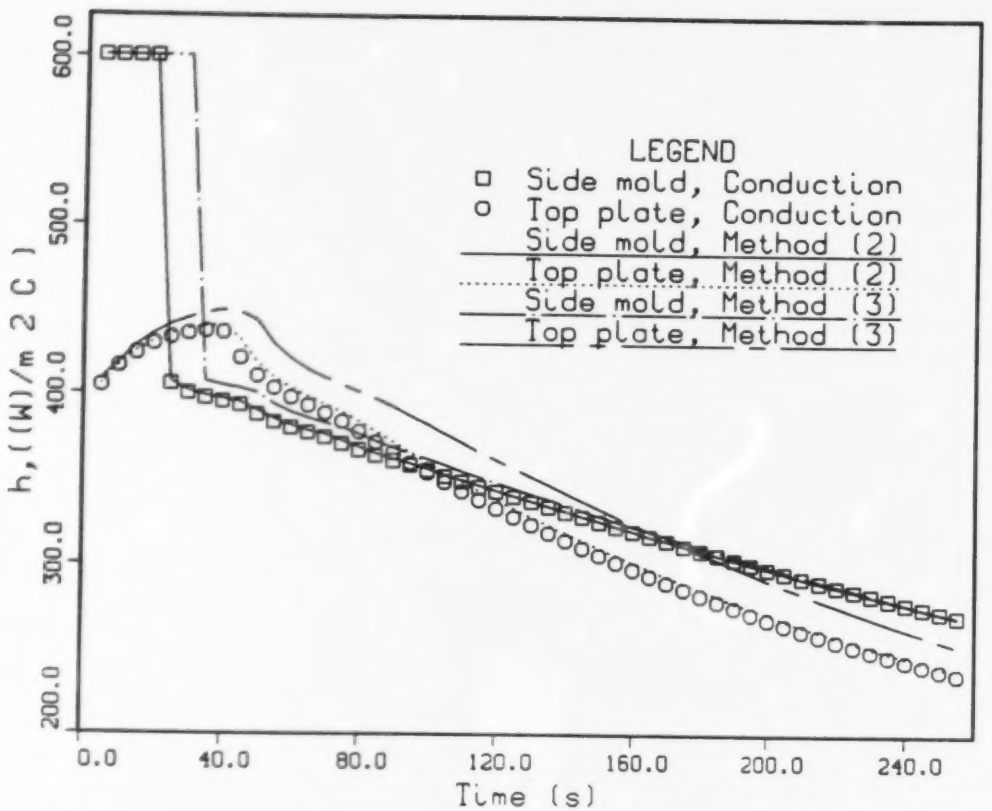

Figure 10 Heat transfer coefficients at the mold casting interface

Appendix
(Main variable names used in the program)

Symbols	Definition
A	Coefficients employed in the TDMA
AB(I,J,K)	Combined convection/diffusion coefficients for 'back' face of control volume, or the coefficient of neighbouring node B
AE(I,J,K)	Combined convection/diffusion coefficients for 'east' face of control volume, or the coefficient of the neighbouring node E
AF(I,J,K)	Combined convection/diffusion coefficients for 'front' face of control volume, or the coefficient of the neighbouring node F
ALAMDA	Length scale factor at inlet of flow domain
ALPHA	AX(I)
ALPHA1	1.0-ALPHA
AN(I,J,K)	Combined convection/diffusion coefficients for 'north' face of control volume, or coefficient of the nieghbouring node N
AP(I,J,K)	Sum of coefficients of combined convective/diffusive flows through all six faces of control volume, or coefficients of the central node P
ARDEN	Area of cell face times density of fluid
ARDENT	Sum of all ARDEN at a cross-section

AREAE	Area of east face of control volume
AREAEW	Area of east/west face of control volume
AREAF	Area of front face of control volume
AREAFB	Area of front/back face of control volume
AREAN	Area of north face of control volume
AREANS	Area of north/south face of control volume
AS(I,J,K)	Combined convection/diffusion coefficients for 'south' face of control volume, or the coefficient of the nieghbouring node S
AW(I,J,K)	Combined convection/diffusion coefficients for 'west' face of control volume, or the coefficient of the neighbouring node W
AX(I)	Axial (or x-) spatial weighting factor (= 0.5*SEW(I)/DXEP(I))
AY(J)	Radial (or y-) spatial weighting factor (= 0.5*SNS(J)/DYNP(J))
AZ(K)	Angular (or z-) spatial weighting factor (= 0.5*SFB(K)/DZFP(K))
BETA	AY(J)
BETA1	1.0-BETA
C	Coefficients employed in the TDMA
C1	Turbulence model constant (= 1.44)
C2	Turbulence model constant (= 1.92)
C3	Turbulence model constant (= 1.0)
CAPPA	Von Karman constant (= 0.4187)
CD	Constant of turbulence model (= 1.0)
CDTERM	(CD*CMU)**0.25
CE(I,J,K)	Mass flows through the 'east' face of control volume
CF(I,J,K)	Mass flows through the 'front' face of control volume

CMU	Constant of trubulence model (= 0.09)
CMU75	CMU**0.75
CN(I,J,K)	Mass flows through the 'north' face of control volume
CP	Maximum of zero and net outflow (SMP) from control volume
CPTIME	Computer time (central processor time) allocation to run
CPTLEF	Total computer time remaining
DE(I,J,K)	Diffusion coefficients through the 'east' face of control volume
DEN(I,J,K)	Local fluid density
DENOLD(I,J,K)	Old time level values of DEN(I,J,K)
DENSIT	Global fluid density
DF(I,J,K)	Diffusion coefficients through the 'front' face of control volume
DITERM	Volume integral of energy dissipation rate in vicinity of walls
DN(I,J,K)	Diffusion coefficients through the 'north' face of control volume
DT	Time step
DU(I,J,K)	Coefficient in u-velocity-correction equation
DUMPR	Control index which specifies whether the dumped data on the disc file are to be read in to resume computations from the next iteration or time step
DUMPW	Control index to govern whether information required to be dumped in disc file for the continuation of next run
DV(I,J,K)	Coefficient in V-velocity-correction equation
DW(I,J,K)	Coefficient in W-velocity-correction equation
DXEP(I)	Axial (or x-) length of mesh distance (= X(I+1)-X(I))
DYNP(J)	Radial (or y-) length of mesh distance (= Y(J+1)-Y(J))

DZFP(K)	Angular (or z-) length of mesh distance (= Z(K+1)-Z(K))
ED(I,J,K)	Local dissipation rate
EDIN	Energy dissipation rate at inlet of flow domain
EDOLD(I,J,K)	Old time level values of ED(I,J,K)
ELOG	Constant of P-function for heat transfer at walls (= 9.793)
FLOREF	Reference mass flow rate used for normalizing residual sources
FLOW	Mass flow rate at an outlet cross-section area based on calculating velocities
FLOWIN	Total mass flow rate through the inlet of flow domain
GACCX	Gravitational acceleration in axial (or x-) direction
GACCY	Gravitational acceleration in radial (or y-) direction
GACCZ	Gravitational acceleration in angular (or z-) direction
GAMH(I,J,K)	Local exchange coefficient, Γ
GAMMA	AZ(K)
GAMMA1	1.0-GAMMA
GE(I,J,K)	Generation of turbulence by shear and direct stresses from mean flow
GENCOU	Part of generation term modified in terms of wall shear stress
GENRES	Total unmodified generation of turbulence minus all shear stress terms at the wall
GREAT	A very large value
H(I,J,K)	Local stagnation enthalpy
HEDU, etc.	Headings for the print out of dependent variable field values
HOLD(I,J,K)	Old time level values of H(I,J,K)
I	Index denoting axial (or x-) position in grid and dependent variable positions

ICOEFF	Control index for the calculation of convection/diffusion coefficients (= 0 coefficients unaltered) (= 1 coefficients fully calculated) (= 2 only diffusion coefficients changed)
IE(J,K)	I indices of the 'east' scalar cell face coinciding with the 'east' boundary of the solution domain according to the radial (or y-) and angular (or z-) directions
IEND(K)	Maximum value of IE(J,K) according to only angular (or z-) direction
IENDJ(J)	Maximum value of IE(J,K) according to only radial (or y-) direction
IVAR	Control index for selection of dependent variables
IMON	I index of the monitoring location where the dependent variables are printed during iteration
INCAL(L)	Control parameters which determines whether the dependent variable L is to be solved
INDCOS	Control index for definition of coordinate system used (= 1 for Cartesian; = 2 for cylindrical)
INDPRI	Number of time steps between print-outs of the dependent variable fields
IPREF	I index of the reference pressure location (i.e. location in the flow domain where relative pressure is held at reference value)
ISTA(K)	Minimum value of IW(J,K) according to only angular (or z-) direction
ISTAJ(J)	Minimum value of IW(J,K) according to only radial (or z-) direction
IT	Declared maximum I-dimension of all variables
ITIME	A running count of the number of time steps performed
ITYPE	Control index for selection of dependent variables
IW(J,K)	I indices of the 'west' scalar cell face coinciding with the 'west' boundary of the solution domain according to the radial (or y-) and angular (or z-) directions

IXSW	Control index for the scan of the block iteration method in the axial (or x-) direction (= 0 one scan; = 2 two scan)
J	Index denoting radial (or y-) position in grid and dependent variables positions
JEND(K)	Maximum value of JN(I,K) according to only angular (or z-) direction
JENDI(I)	Maximum value of JN(I,K) according to only axial (or x-) direction
JMON	J index of the monitoring location where the dependent variables are printed during iteration
JN(I,K)	J indices of the 'north' scalar cell face coinciding with the 'north' boundary of the solution domain according to the axial (or x-) and angular (or z-) directions
JPREF	J index of the reference pressure location (i.e. location in the flow domain where relative pressure is held at reference value)
JS(I,K)	J indices of the 'south' scalar cell face coinciding with the 'south' boundary of the solution domain according to the axial (or x-) and angular (or z-) directions
JSTA(K)	Minimum value of JS(I,K) according to only angular (or z-) direction
JSTAI(I)	Minimum value of JS(I,K) according to only axial (or x-) direction
JT	Declared maximum J-dimension of all variable
JYSW	Control index for the scan of the block iteration method in the radial (or y-) direction (= 0 one scan; = 2 two scan)
K	Index denoting angular (or z-) position in grid and dependent variable positions
KB(I,J)	K indices of the 'back' scalar cell face coinciding with the 'back' boundary of the solution domain according to the axial (or x-) and radial (or z-) directions

KF(I,J)	K indices of the 'front' scalar cell face coinciding with the 'front' boundary of the solution domain according to the axial (or x-) and radial (or y-) directions
KMON	K index of the monitoring location where the dependent variables are printed during iteration
KPREF	K index of the reference pressure location (i.e. location in the flow domain where relative pressure is held at reference value)
KT	Declared maximum K-dimension of all variables
KZSW	Control index for the scan of the block iteration method in the angular (or z-) direction (= 0 one scan; = 2 two scan)
LAMIN	Control index specifying whether the k-ε equations are solved
LED	Index for the energy dissipation equation
LEN	Index for the thermal energy equation
LP	Index for the pressure-correction equation
LPROPS	Additional index for the fluid properties updated
LTE	Index for the turbulent kinetic energy equation
LU	Index for the axial (or x-) momentum equation
LV	Index for the radial (or y-) momentum equation
LW	Index for the angular (or z-) momentum equation
MAXIT	Maximum number of iterations allowed per time step, or to be completed if iteration sequence is not stopped by test on value of source
MFIX	Control index determining what kine of cross-sectional plane that the results are printed (= 1 x-y plane; = 2 x-z plane; = 3 y-z plane)
MTAPE	Control index for dumping results onto magnetic tape
MTAPEO	Control index to govern whether the tape must advance for unsteady problems or the data from previous run stored on a magnetic tape for steady problem (If the present run is a continuation run of the unsteady problems, athe tape must be advanced to the end of previous written data.)

NDIMEN	Number of dimensions of the calculation domain
NI	Maximum values of IEND(K) and IENDJ(J)
NIM1	
NITER	A running count of the number of iterations performed
NIU	NI-1
NIUM1	NIU-1
NJ	Maximum values of JEND(K) and JENDI(I)
NJM1	
NJV	NJ-1
NJVM1	NJV-1
NK	Maximum values of KB(I,J) and KF(I,J)
NKM1	
NKW	NK-1
NKWM1	NKW-1
NP or NPLANE	Control index determining on which cross-sectional plane that the results are printed
NSWP(L)	Number of inner (or block) iterations on the L dependent variable equations
NTAPE	Control index determining the number of time steps after which results are written onto magnetic tape
NWRITE	A running count of the number of tape writes
P(I,J,K)	Local pressure
PATM	Atmospheric pressure
PFUN	Constant in heat transfer wall-function
PHI(I,J,K)	General representation for all dependent variables
PI	4.0*ATAN(1.0)
PP(I,J,K)	Pressure-correction values in the field

PPLUS	Correction to the reference pressure PPREF, and reference pressure correction
PPREF	Reference pressure
PRL(I,J,K)	Local laminar Prandtl number
PRT(I,J,K)	Local turbulent Prandtl number
PRLED	Laminar Schmidt number in the dissipation rate equation
PRLTE	Laminar Schmidt number in the turbulence energy equation
PRTED	Turbulent Schmidt number in the dissipation rate equation
PRTTE	Turbulent Schmidt number in the turbulence energy equation
R(J)	Radius (= 1 if Cartesian coordinate is used) of main grid node from symmetry axis
RADIUS	Radius of the domain
RDT	Temporal term
RESOR(L)	Sum of residual sources within calculation domain for any dependent variable L equations
RESOR1	Local residual for any dependent variable
RT	Available computer time (CPU time) for further iteration or time step
RT0	CPU time at the start of the calculation
RT1	CPU time at the start of the time step being calculated
RT2	CPU time at the end of the time step being calculated or at the start of the iteration being calculated
RT3	CPU time at the end of the iteration being calculated
RTMIN	Estimated computer time (CPU time) consumed for one iteration or time step, to be specified by the user
RV(J)	Radius (= 1 if Cartesian coordinate is used) of location of radial velocity from symmetry axis
SMALL	A very small number

SEW(I)	XU(I)-XU(I-1)
SFB(K)	ZW(K)-ZW(K-1)
SMAX	Maximum normalized residuals possible in the solution
SMP	Net outflow from control volume
SNORM(L)	A reference quantity for the normalized residual source of any dependent variable L equations
SNS(J)	YV(J)-YV(J-1)
SORMAX	Level of the normalized residuals below which iteration procedure is taken as converged
SOURCE	Maximum of the residuals of all dependent variables of interest
SP(I,J,K)	Coefficient S_p of the linearized source in the finite volume equations
SSB(I,J)	Wall shear stress coefficient at the 'back' boundary
SSBT(I,J)	Heat transfer coefficient at the 'back' boundary
SSE(J,K)	Wall shear stress coefficient at the 'east' boundary
SSET(J,K)	Heat transfer coefficient at the 'east' boundary
SSF (I,J)	Wall shear stress coefficient at the 'front' boundary
SSFT(I,J)	Heat transfer coefficient at the 'front' boundary
SSN(I,K)	Wall shear stress coefficient at the 'north' boundary
SSNT(I,K)	Heat transfer coefficient at the 'north' boundary
SSS(I,K)	Wall shear stress coefficient at the 'south' boundary
SSST(I,K)	Heat transfer coefficient at the 'south' boundary
SSW(J,K)	Wall shear stress coefficient at the 'west' boundary
SSWT(J,K)	Heat transfer coefficient at the 'west' boundary
STEADY	Control index specifying whether the solution required is steady transport processes
SU(I,J,K)	S_u of the linearized source in the finite volume equations

TE(I,J,K)	Local turbulence kinetic energy
TEIN	Turbulent energy at inlet of flow domain
TEOLD(I,J,K)	Old time level values of TE(I,J,K)
TERM	CMU75/CAPPA
TFIXB	Control index for the constant wall temperature condition at 'back' boundary
TFIXE	Control index for the constant wall temperature condition at 'east' boundary
TFIXF	Control index for the constant wall temperature condition at 'front' boundary
TFIXN	Control index for the constant wall temperature condition at 'north' boundary
TFIXS	Control index for the constant wall temperature condition at 'south' boundary
TFIXW	Control index for the constant wall temperature condition at 'west' boundary
TIME	Actual time (problem) in seconds being calculated
TMAX	Maximum time to be calculated
TURBIN	Turbulent intensity factor at inlet of flow domain
U(I,J,K)	Local axial (or x-) velocity
UOLD(I,J,K)	Old time level values of U(I,J,K)
UPLUS	Local friction velocity at wall boundary of flow domain
URF(L)	Under-relaxation factors of any dependent variable L
URFVIS	Under-relaxation factor of viscosity
V(I,J,K)	Local radial (or y-) velocity
VIN	Velocity at inlet of flow domain
VINC	Uniform increment of normal velocity at outlet of flow domain
VIS(I,J,K)	Local effective viscosity

VISCAL	Value of effective viscosity before under-relaxation
VISCOS	Global effective or laminar viscosity
VISL(I,J,K)	Local laminar viscosity
VOL	Volume of control volume
VOLD(I,J,K)	Old time level values of V(I,J,K)
W(I,J,K)	Local angular (or z-) velocity
WALLB	Control index specifying whether the 'back' boundary is wall
WALLE	Control index specifying whether the 'east' boundary is wall
WALLF	Control index specifying whether the 'front' boundary is wall
WALLN	Control index specifying whethe the 'north' boundary is wall
WALLS	Control index specifying whethe the 'south' boundary is wall
WALLW	Control index specifying whether the 'west' boundary is wall
WOLD(I,J,K)	Old time level values of W(I,J,K)
WV(I)	Spatial weighting factors equal to 0.5
X(I)	Axial (or x-) coordinate positions of the grid lines
XP	Axial (or x-) distance from the nearest inner grid point to the wall
XU(I)	x-coordinate values of the axial (or x-) velocity locations
Y(J)	Radial (or y-) coordinate positions (measured from symmetry axis) of the grid lines
YP	Radial (or y-) distance from the nearest inner grid point to the wall
YPLUSB	Local Reynolds number based on friction velocity and distance from 'back' wall-boundary of flow domain

YPLUSE	Local Reynolds number based on friction velocity and distance from 'east' wall-boundary of flow domain
YPLUSF	Local Reynolds number based on friction velocity and distance from 'front' wall-boundary of flow domain
YPLUSN	Local Reynolds number based on friction velocity and distance from 'north' wall-boundary of flow domain
YPLUSS	Local Reynolds number based on friction velocity and distance from 'south' wall-boundary of flow domain
YPLUSW	Local Reynolds number based on friction velocity and distance from 'west' wall-boundary of flow domain
YV(J)	y-coordinate values of the radial (or y-) velocity locations
Z(K)	Angular (or z-) coordinate positions of the grid lines
ZP	Angular (or z-) distance from the nearest inner grid point to the wall
ZW(K)	z-coordinate values of the angular (or z-) velocity locations